
Probability Distribution Learning Framework and Its Application in Deep Learning

Binchuan Qi*

College of Electronics and Information Engineering
Tongji University
Shanghai, China
2080068@tongji.edu.cn

Wei Gong

College of Electronics and Information Engineering
Tongji University, China
weigong@tongji.edu.cn

Li Li

College of Electronics and Information Engineering
Tongji University, China
lili@tongji.edu.cn

Abstract

This paper aims to elucidate the theoretical mechanisms underlying deep learning from a probability distribution estimation perspective, with Fenchel-Young Loss serving as the loss function. In our approach, the learning error, which measures the discrepancy between the model's predicted distribution and the posterior expectation of the true unknown distribution given sampling, is formulated as the primary optimization objective. Therefore, the learning error can be regarded as the posterior expectation of the expected risk. As many important loss functions, such as Softmax Cross-Entropy Loss and Mean Squared Error Loss, are specific instances of Fenchel-Young Losses, this paper further theoretically demonstrates that Fenchel-Young Loss is a natural choice for machine learning tasks, thereby ensuring the broad applicability of the conclusions drawn in this work. In the case of using Fenchel-Young Loss, the paper proves that the model's fitting error is controlled by the gradient norm and structural error, thereby providing new insights into the mechanisms of non-convex optimization and various techniques employed in model training, such as over-parameterization and skip connections. Furthermore, it establishes model-independent bounds on the learning error, demonstrating that the correlation between features and labels (equivalent to mutual information) controls the upper bound of the model's generalization error. Ultimately, the paper validates the key conclusions of the proposed method through empirical results, demonstrating its practical effectiveness.

*Use footnote for providing further information about author (webpage, alternative address)—*not* for acknowledging funding agencies.

1 Introduction

Alongside the remarkable practical achievements of deep learning, several fundamental questions regarding deep learning remain unanswered within the classical learning theory framework. These include the mechanisms underlying the optimization of non-convex, non-linear, and often non-smooth objectives, how the number of parameters impacts model performance, and how deep neural networks (DNNs) manage to avoid overfitting despite their vast capacity.

Challenge. In deep learning, first-order optimization methods—such as gradient descent (GD) [1] and stochastic gradient descent (SGD) [2]—are extensively utilized to address the non-convex optimization challenges intrinsic to model training [3, 4]. Within the classical optimization theoretical framework, these algorithms are generally anticipated to converge to a stationary point, which may be a local minimum, a local maximum, or a saddle point [5, 6]. Additionally, numerous non-convex problems with seemingly simple structures have been demonstrated to be NP-hard, such as Standard Quadratic Programming (StQP) and copositivity testing [7–10]. However, extensive empirical evidence indicates that first-order optimization methods can effectively identify approximate global optima for the highly complex and non-convex optimization landscapes encountered in deep learning [11–15].

Key insights from studies [16–19] highlight the critical role of over-parameterization in achieving global optima and improving the generalization capabilities of DNNs. Recent research has demonstrated that the evolution of trainable parameters in continuous-width DNNs during training can be effectively described by the neural tangent kernel (NTK) [20–25] and mean-field theory [26–29]. However, in practical scenarios where neural networks have finite widths, it remains uncertain whether NTK theory and mean-field theory can sufficiently characterize the convergence properties of such networks [30]. It is widely accepted that the inherent stochasticity of stochastic optimization algorithms introduces implicit regularization, steering model parameters toward flat minima [31–34]. This phenomenon is believed to influence the model’s generalization and fitting performance. Nevertheless, it has been noted that flatness can be artificially manipulated without altering the model’s output [35]. This observation suggests that the notion of flat minima as a reliable indicator of strong generalization and fitting ability may not be as straightforward or universally applicable as initially assumed. The studies by [11, 12, 14, 15] demonstrate that high-capacity DNNs can still generalize well with genuine labels, yet generalize poorly when trained with random labels. This apparent contradiction with the traditional understanding of overfitting [36, 37] in complex models also highlights the need for further investigation [38, 39].

Motivation. A substantial proportion of machine learning tasks can be conceptualized within the domain of probability distribution estimation. Supervised classification and regression tasks are mathematically characterized by the process of learning the conditional probability distribution of labels given input features. Generative learning involves estimating the underlying joint distribution of features. Consequently, adopting a perspective of probability distribution estimation for both machine learning and deep learning is a logical and coherent choice.

Contribution. The contributions of this paper are stated as follows.

1. This paper models machine learning tasks as the estimation of underlying distributions given the available sample set. The underlying distributions are modeled as random variables within the probability simplex, with the learning error formulated as the optimization objective. The learning error measures the discrepancy between the model’s predicted distribution and the posterior expectation of the possible true distributions under the given sample set. Therefore, the learning error can be regarded as the posterior expectation of the expected risk. Under the equal-probability hypothesis, the learning error for any model is computable, which represents a key distinction from the expected risk in traditional statistical machine learning frameworks.

2. This paper demonstrates that although fitting a model to the empirical distribution involves a non-convex optimization problem, when using Fenchel-Young Loss, its global optimum can be achieved by reducing the gradient norm and structural error. The gradient norm can be iteratively optimized through SGD, and this paper further shows that techniques such as random parameter initialization, over-parameterization, dropout, and skip connections can reduce the structural error. Thus, this provides new theoretical insights into the mechanisms of non-convex optimization in deep learning.

3. This paper establishes model-independent bounds on the learning error. These bounds demonstrate that uncertainty serves as a lower bound for the learning error, while the correlation between features and labels (or mutual information) governs the upper bound of the learning error. Consequently, it follows that in the absence of any information beyond the sampled data, the learning error is theoretically always present and can be quantified by uncertainty. The greater the mutual information between features and labels, the higher the upper bound of the learning error, implying a larger posterior expectation of the expected risk. Since the learning error encompasses both the model’s fitting error and generalization error, this paper provides new insights into the generalization capability of models.
4. Key findings from this approach are validated through experimental results, demonstrating their practical effectiveness.

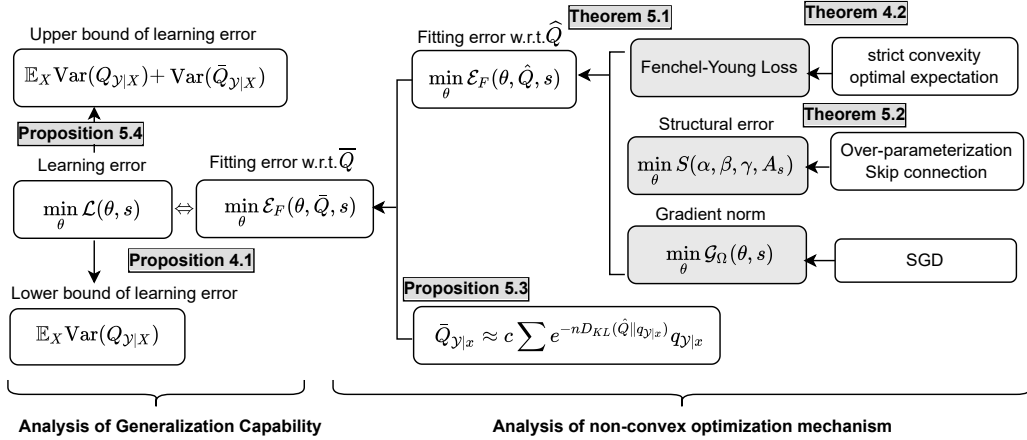


Figure 1: Optimization Strategies of PD estimation.

The core theorems of this paper, along with their logical relationships, are illustrated in Figure 1. This study focuses on learning error as the optimization objective. Proposition 4.1 demonstrates that the learning error can be decomposed into two components: a model-independent term called Uncertainty and the fitting error of the model with respect to \bar{Q} . Consequently, optimizing the fitting error, denoted as $\mathcal{L}_F(\theta, \bar{Q}, s)$, becomes the central challenge. Proposition 5.3 and Proposition 5.4 establish that $\min \mathcal{L}_F(\theta, \hat{Q}, s)$ can approximate $\min \mathcal{L}_F(\theta, \bar{Q}, s)$, with the approximation error being determined by the size of the training set and the correlation (or mutual information) between features and labels ($\text{Var}(\bar{Q}_{y|X})$ or $I(X; Y)$). Theorem 5.1 shows that, although minimizing $\mathcal{L}_F(\theta, \hat{Q}, s)$ is a non-convex optimization problem, when using the Fenchel-Young Loss, both the upper and lower bounds of $\mathcal{L}_F(\theta, \hat{Q}, s)$ can be controlled by reducing the gradient norm and the structural error. SGD naturally reduces the gradient norm, while Theorem 5.2 proves that increasing the number of parameters under the condition of gradient independence reduces the structural error. These findings provide theoretical insights into the mechanisms of non-convex optimization in deep learning. Theorem 4.2 proves that any loss function satisfying two natural properties for machine learning tasks—strict convexity and optimal expectation—is equivalent to the Fenchel-Young Loss. This ensures that the conclusions drawn in this study, based on the use of the Fenchel-Young Loss, are general and widely applicable. Finally, Proposition 5.4 reveals that the lower bound of the learning error is determined by Uncertainty, while the upper bound is influenced by the correlation or mutual information between features and labels.

Organization. The paper is organized as follows: Section 2 reviews the research progress and current status. Fundamental concepts are defined in Section 3. The proposed method and its application are detailed in Section 4 and Section 5. Experimental settings and results are presented in Section 6. The conclusions are summarized in Section 7. Lemmas supporting the theorems and all proofs are provided in Section A and Section B, respectively. A broader review of related work is included in Section C. For ease of reading, a summary of the notation used throughout this paper is provided in Section D.

2 Related Work

It is widely accepted that the inherent stochasticity of stochastic optimization algorithms, such as SGD, performs implicit regularization, guiding parameters towards flat minima [31–34]. This tendency towards flat minima is believed to influence the model’s generalization and fitting performance positively. Flat minima are generally considered to generalize better than sharp (non-flat) minima [40]. To identify flat minima, various mathematical definitions of flatness have been proposed. A prevalent definition involves examining the largest eigenvalue (λ_{\max}) of the Hessian matrix of the loss function with respect to the model parameters on the training set [41, 42]. In response to the importance of finding flat minima, Sharpness-Aware Minimization (SAM) is introduced, which is specifically designed to seek out these flat solutions [43]. However, it is demonstrated that, while keeping the model’s output unchanged, flatness can be "freely" altered through reparametrizing the models [35]. This observation contradicts experimental results that suggest flatness impacts a model’s generalization and fitting performance. As of now, the theoretical mechanisms underlying this phenomenon have not been fully elucidated.

Research has found that over-parameterization plays a pivotal role in finding the global optimum and enhancing the generalization ability of deep neural networks (DNNs) [17–19]. Therefore, analyzing the optimization mechanisms of deep learning from the perspective of model parameter scale has become an important research direction. The NTK has thus emerged as a pivotal concept, as it captures the dynamics of over-parameterized neural networks trained by GD [20]. It is already known in the literature that DNNs in the infinite width limit are equivalent to a Gaussian process [44–48]. It has been elucidated that the evolution of the trainable parameters in continuous-width DNNs during training can be captured by the NTK [20]. Some work has shown that with a specialized scaling and random initialization, the parameters of continuous-width two-layer DNNs are restricted to an infinitesimal region around the initialization and can be regarded as a linear model with infinite-dimensional features [17, 49, 21, 23]. Since the system becomes linear, the dynamics of GD within this region can be tracked via properties of the associated NTK, and the convergence to the global optima with a linear rate can be proved. Later, the NTK analysis of global convergence was extended to multi-layer neural nets [50, 22, 51, 24, 52]. An alternative research direction attempts to examine the infinite-width neural network from a mean-field perspective [26–29]. The key idea is to characterize the learning dynamics of noisy SGD as the gradient flows over the space of probability distributions of neural network parameters. As time approaches infinity, the noisy SGD converges to the unique global optimum of the convex objective function for the two-layer neural network with continuous width. NTK and mean-field methods provide a fundamental understanding on training dynamics and convergence properties of non-convex optimization in infinite-width neural networks. However, the assumption of infinitely wide neural networks does not hold in real-world applications, making it an open question whether NTK and mean-field theories can be applied to the analysis of practical neural networks. Some recent research findings [53, 54] indicate that the NTK theory does not generally describe the training dynamics of finite-width DNNs accurately and suggest that an entirely new conceptual viewpoint is required to provide a full theoretical analysis of DNNs’ behavior under GD.

In summary, there remains a lack of clarity in understanding why, for certain algorithms and datasets, increasing the number of parameters actually enhances performance and generalization [39]. The available body of evidence suggests that classical tools from statistical learning theory alone may be insufficient to fully explain the behavior of DNNs [12, 55].

3 Preliminaries

3.1 Notation

1. Random variables are denoted using upper case letters such as Z , X , and Y , which take values in sets \mathcal{Z} , \mathcal{X} and \mathcal{Y} , respectively. \mathcal{X} represents the input feature space and \mathcal{Y} denotes a finite set of labels. The cardinality of set \mathcal{Z} is denoted by $|\mathcal{Z}|$.

2. We utilize the notation f_θ (hereinafter abbreviated as f) to denote the model characterized by the parameter vector θ . Additionally, $f_\theta(x)$ (abbreviated as $f(x)$) represents the model with a parameter vector θ and a specific input x . The space of models, which is a set of functions endowed with some structure, is represented by $\mathcal{F}_\Theta = \{f_\theta : \theta \in \Theta\}$, where Θ denotes the parameter space. Similarly,

we define the hypothesis space with feature x as $\mathcal{F}_\Theta(x) := \{f_\theta(x) : \theta \in \Theta\}$. We use $g(\theta)$ to denote a model with constant output, which corresponds to the native probability distribution estimation discussed below.

3. The Legendre-Fenchel conjugate of a function Ω is denoted by $\Omega^*(\nu) := \sup_{\mu \in \text{dom}(\Omega)} \langle \mu, \nu \rangle - \Omega(\mu)$ [56]. By default, Ω is a continuous strictly convex function, and its gradient with respect to μ is denoted by $\nabla_\mu \Omega(\mu)$. For convenience, we use μ_Ω^* to represent $\nabla_\mu \Omega(\mu)$. When $\Omega(\cdot) = \frac{1}{2} \|\cdot\|_2^2$, we have $\mu = \mu_\Omega^*$. The Fenchel-Young loss $d_\Omega : \text{dom}(\Omega) \times \text{dom}(\Omega^*) \rightarrow \mathbb{R}_{\geq 0}$ generated by Ω is defined as [57]:

$$d_\Omega(\mu, \nu) := \Omega(\mu) + \Omega^*(\nu) - \langle \mu, \nu \rangle, \quad (1)$$

where Ω^* denotes the conjugate of Ω .

4. The maximum and minimum eigenvalues of matrix A are denoted by $\lambda_{\max}(A)$ and $\lambda_{\min}(A)$, respectively.

5. To improve clarity and conciseness, we transform the distribution function into a vector for processing and provide the following definitions of symbols:

$$\begin{aligned} q_{\mathcal{X}} &:= (q_{\mathcal{X}}(x_1), \dots, q_{\mathcal{X}}(x_{|\mathcal{X}|}))^\top, \\ q_{\mathcal{Y}|x} &:= (q_{\mathcal{Y}|X}(y_1|x), \dots, q_{\mathcal{Y}|X}(y_{|\mathcal{Y}|}|x))^\top. \end{aligned} \quad (2)$$

Here, $q_{\mathcal{X}}(x)$ and $q_{\mathcal{Y}|X}(y|x)$ represent the marginal and conditional PMFs/PDFs, respectively. In this paper, we use $\mathbb{E}_{X \sim q_{\mathcal{X}}} f(X)$ to denote the expectation of $f(X)$ with respect to the distribution $q_{\mathcal{X}}$.

3.2 Setting and Basics

The random pair $Z = (X, Y)$ follows the true underlying distribution q and takes values in the product space $\mathcal{Z} = \mathcal{X} \times \mathcal{Y}$. In this study, it is assumed by default that both $|\mathcal{X}|$ and $|\mathcal{Y}|$ are of finite dimensions. The sample or training data, denoted by an n -tuple $s^n := \{z^{(i)}\}_{i=1}^n = \{(x^{(i)}, y^{(i)})\}_{i=1}^n$, is composed of i.i.d. samples drawn from the unknown true distribution $q_{\mathcal{Z}}$ (abbreviated as q). Given the available information, the true underlying distribution is indeterminate. In other words, although q does indeed exist uniquely as the true distribution, it cannot be uniquely determined based on the existing information. Consequently, we model q as a random variable Q in the probability simplex space Δ . Thus, the central focus of this study is to minimize the expected loss between the distribution predicted by the model and Q under a specific metric. Let $\mathcal{Q}^{(s^n, \mathcal{P})}$ (abbreviated as \mathcal{Q}) denote the posterior distribution of Q , conditional on the independent and identically distributed (i.i.d.) sample dataset s^n and the prior distribution \mathcal{P} . The unknown true conditional distribution $q_{\mathcal{Y}|x}$ is modeled as a random variable in probability simplex $\Delta^{|\mathcal{Y}|}$ with distribution $\mathcal{Q}_{\mathcal{Y}|x}$. We define $\bar{Q} = \mathbb{E}_{Q \sim \mathcal{Q}} Q$. In the absence of prior knowledge about Q , one can estimate \bar{Q} using event frequencies. This empirical probability distribution based on s is represented by $\hat{Q}(s^n) := \frac{1}{n} \sum_{i=1}^n \mathbf{1}_{\{z\}}(z^{(i)})$, which is referred to as the empirical probability distribution.

In the absence of further information regarding the i.i.d. sample s^n for q , we adopt the equal-probability hypothesis, which assumes that \mathcal{P} is a uniform distribution across the space Δ . This hypothesis is foundational in statistical physics, suggesting that probabilities are evenly distributed over the space Δ . Unless otherwise specified, this study assumes that the prior distribution \mathcal{P} for all distributions is uniform.

It is crucial to note that given the sample dataset s^n , calculating \bar{Q} and \mathcal{Q} becomes feasible. When $Q = q$, the empirical probability distribution \hat{Q} , inferred from the sample s^n , follows a multinomial distribution: $n\hat{Q} \sim \text{multinomial}(n, q)$. Consequently, using Bayes's theorem, we can derive:

$$\mathcal{Q}(q) = \Pr(Q = q | s^n) = \frac{\Pr(s^n, q)}{\sum_{q' \in \Delta} \Pr(s^n, q')}. \quad (3)$$

Here, $n_z = \sum_{i=1}^n \mathbf{1}_{\{z\}}(z^{(i)})$ represents the count of occurrences of z in the sample set s^n , $\Pr(s^n, q') = \mathcal{P}(q') n! \prod_{z \in \mathcal{Z}} \frac{q'(z)^{n_z}}{n_z!}$ denotes the probability of observing the sample s^n given the distribution q' , with $\mathcal{P}(q') = \frac{1}{|\Delta|}$. For the calculation of $\mathcal{Q}_{\mathcal{Y}|x}$, a similar approach can be applied.

4 Problem formulation and loss function

4.1 Learning error as the objective

Given that many machine learning tasks fundamentally involve estimating underlying probability distributions, and these distributions cannot be uniquely determined based on the available information, we model the probability distribution as a random variable within the probability simplex. Thus, we first define the following learning error as the optimization objective, where all distributions are considered as random variables in the probability simplex.

Definition 4.1 (Learning Error) Let $p_{Y|x}(\theta)$ represent the model's predicted conditional probability distribution of Y given $X = x$. The learning error is then defined as follows:

$$\mathcal{L}(\theta, s) = \mathbb{E}_{Q_X \sim \mathcal{Q}_X} \mathbb{E}_{X \sim Q_X} \mathbb{E}_{Q_{Y|X} \sim \mathcal{Q}_{Y|X}} \|Q_{Y|X} - p_{Y|X}(\theta)\|_2^2 \quad (4)$$

where:

- Q_X and $Q_{Y|x}$ are the posterior distributions of Q_X and $Q_{Y|x}$, respectively, given the sample s .
- $\mathbf{1}_y$ is an indicator function that represents the one-hot encoding of the label y .

The function $\mathcal{L}(\theta, s)$ describes the error between the model's predicted distribution and the plausible distributions under the posterior expectation given a sample s . Therefore, the learning error can be regarded as the posterior expectation of the expected risk. We thus formulate the optimization objectives for PD estimation as follows:

$$\min_{\theta} \mathcal{L}(\theta, s), \quad (5)$$

where θ corresponds to the learnable parameters of the model, $s = \{z_i\}_{i=1}^n$ denotes the dataset consisting of n i.i.d. samples.

The definition of the learning error appears complex. However, by employing the Bias-Variance Decomposition, we derive the following proposition:

Proposition 4.1

$$\mathcal{L}(\theta, s) = \mathbb{E}_{X \sim \bar{Q}_X} \text{Var}(Q_{Y|X}) + \mathbb{E}_{X \sim \bar{Q}_X} \|\bar{Q}_{Y|X} - p_{Y|X}(\theta)\|_2^2, \quad (6)$$

where $\text{Var}(Q_{Y|X}) = \mathbb{E}_{Q_{Y|X} \sim \mathcal{Q}_{Y|X}} \|Q_{Y|X} - \bar{Q}_{Y|X}\|_2^2$.

The proof of this proposition is provided in Appendix B.2. Proposition 4.1 highlights the decomposition of the learning error into two components: a variance term and a bias term. Specifically, the term $\mathbb{E}_{X \sim \bar{Q}_X} \|\bar{Q}_{Y|X} - p_{Y|X}(\theta)\|_2^2$ is analogous to the expected risk under Mean Squared Error (MSE) Loss, $\mathbb{E}_{X \sim q_X} \|q_{Y|X} - p_{Y|X}(\theta)\|_2^2$. The interpretation of these terms is also similar: The former requires the model's predicted distribution $p_{Y|X}(\theta)$ to approximate the posterior expectation $\bar{Q}_{Y|x}$; the latter requires the model's predictions to approximate the underlying unknown true distribution $q_{Y|x}$. From the perspective of probability distribution estimation, $\bar{Q}_{Y|x}$ represents a reasonable estimate of $q_{Y|x}$ given the sampled data s . Therefore, the term $\mathbb{E}_{X \sim \bar{Q}_X} \|\bar{Q}_{Y|X} - p_{Y|X}(\theta)\|_2^2$ in the learning error essentially substitutes the unknown true distribution $q_{Y|x}$ with its posterior expectation $\bar{Q}_{Y|x}$. Therefore, **the learning error can be regarded as the posterior expectation of the expected risk.**

On the other hand, the learning error $\mathcal{L}(\theta, s)$ and the expected risk $\mathbb{E}_{X \sim q_X} \|q_{Y|X} - p_{Y|X}(\theta)\|_2^2$ exhibit several profound differences:

1. Computability: Since Q_X and $Q_{Y|x}$ can be computed given sample s , both $\bar{Q}_{Y|x}$ and \bar{Q}_X can be accurately calculated. This means that the learning error defined in Proposition 4.1 can theoretically be calculated for any model. This contrasts with traditional statistical machine learning where the true underlying distribution $q_{Y|x}$ is unknown and cannot be directly computed.

2. Lower Bound on Learning Error: Because $\mathbb{E}_{X \sim \bar{Q}_X} \|\bar{Q}_{Y|X} - p_{Y|X}(\theta)\|_2^2$ is non-negative, $\mathbb{E}_{X \sim \bar{Q}_X} \text{Var}(Q_{Y|X})$ serves as a lower bound for the learning error. Importantly, $\mathbb{E}_{X \sim \bar{Q}_X} \text{Var}(Q_{Y|X})$

is model-independent. Thus, the form of the learning error provides a model-independent lower bound that solely depends on the sampled data. This indicates that regardless of the model used, the learning error has a unique lower bound determined only by the sampling data.

3. Theoretical Optimizability: In deep learning, the expected risk with respect to model parameters is often non-convex or even non-smooth. Despite this, empirical evidence suggests that simple first-order gradient methods, such as SGD, are effective. Traditional optimization theory struggles to explain this phenomenon. However, in the context of using the Fenchel-Young Loss, we will theoretically demonstrate that SGD can ensure convergence of the above learning error. This theoretical foundation supports the practical effectiveness of using SGD for optimizing models under the Fenchel-Young Loss framework.

4.2 Fenchel-Young Loss as the loss function

In machine learning, loss functions play a pivotal role. Different loss functions can significantly impact the learning performance, affecting aspects like convergence speed, robustness, and generalization ability. To ensure that the conclusions drawn from this study are broadly applicable and not tied to a specific choice of loss function, we opt for the Fenchel-Young loss, a generalized form of loss function. In this section, we delve into the rationale behind adopting the Fenchel-Young loss both in practical applications and theoretical analyses, illustrating why it constitutes a reasonable choice.

As shown in Table 1, it is found that a majority of loss functions widely used in real-world scenarios can be expressed as Fenchel-Young Losses [57]. In this subsection, we further demonstrate the theoretical generality of Fenchel-Young Losses. Specifically, we show that when a loss function possesses strict convexity and the optimal expectation, this loss function is equivalent to a Fenchel-Young Loss. This equivalence ensures that the conclusions derived in this paper based on Fenchel-Young Losses have both theoretical generality and practical applicability.

First, we define the two conditions: strict convexity and optimal expectation. The **strict convexity** condition implies that the loss function ℓ must be strictly convex with respect to the model’s predicted distribution p . Clearly, this condition naturally aligns with the requirements of machine learning; when a loss function has multiple optima, it becomes ambiguous to learn a specific target by minimizing the loss. The **optimal expectation** condition stipulates that the expected loss, $\mathbb{E}_Q[\ell(Q, p)]$, reaches its global minimum value when $p = \mathbb{E}_Q[Q] = \bar{Q}$. Formally, this condition can be expressed as:

$$\mathbb{E}_Q[Q] = \arg \min_p \mathbb{E}_Q[\ell(Q, p)]. \quad (7)$$

This condition ensures that the loss function effectively guides the model towards the expectation of the learning target. According to the (Weak) Law of Large Numbers, these conditions ensure that we can approximate the expectation of the true distribution by fitting the empirical distribution; hence, they constitute a natural requirement for distribution learning. In noisy supervised learning scenarios, this concept becomes particularly intuitive: when Q is noisy, we ideally want the model to learn \bar{Q} , the expected value of the targets. Therefore, these two conditions—strict convexity and optimal expectation—are natural choices for machine learning tasks. The loss functions considered in this paper need to satisfy only these two conditions, ensuring that our conclusions possess theoretical generality and are broadly applicable across various learning scenarios.

Theorem 4.2 *Given that the loss function $\ell(q, p)$ satisfies the two conditions of strict convexity and optimal expectation, there exists a strictly convex function Ω such that:*

$$\ell(q, p) - \ell(q, q) = d_\Omega(q, p_\Omega^*). \quad (8)$$

The proof of this result is provided in Appendix B.3. The theorem demonstrates that any loss function $\ell(q, p)$ satisfying the two key conditions—strict convexity and optimal expectation—can be equivalently expressed in terms of $d_\Omega(q, p_\Omega^*)$. Taking the Softmax Cross-Entropy Loss as an example, the corresponding Fenchel-Young Loss can be expressed as:

$$\ell_{CE}(q, p) - \ell_{CE}(q, q) = D_{\text{KL}}(y \| p) = d_\Omega(y, f_\theta(x)), \quad (9)$$

where $\Omega(p) = -H(p)$ is the negative entropy of p , $p = (f_\theta(x))_{\Omega^*}^* = \text{Softmax}(f_\theta(x))$ represents the probability distribution obtained by applying the softmax function to $f_\theta(x)$, $\ell_{CE}(\cdot, \cdot)$ denotes the

Cross-Entropy Loss function. In summary, the use of Fenchel-Young Loss not only ensures alignment with practical applications but also offers valuable theoretical insights. Furthermore, in the following sections, we will demonstrate how the Fenchel-Young Loss facilitates the analysis of deep learning.

Therefore, in this paper, we use the Fenchel-Young Loss as the loss function to guide the iterative optimization of the model. The empirical loss on the sample s is defined as $\mathbb{E}_X d_\Omega(\hat{Q}_{Y|X}, f_\theta(x))$, where $X \sim \hat{Q}$, and $f_\theta(x)$ represents the output of the model. The predicted distribution of the model is given by $p_{Y|x} = (f_\theta(x))_{\Omega^*}^*$, where $(\cdot)_{\Omega^*}^*$ denotes the transformation induced by the Fenchel conjugate associated with the function Ω . Therefore, in our study, the empirical risk of classification tasks takes the form:

$$\mathbb{E}_{XY \sim \hat{Q}} d_\Omega(\mathbf{1}_Y, f_\theta(X)). \quad (10)$$

4.3 Basic definitions

To articulate our approach, we list the definitions used in our method as follows:

1. Fitting Error. The fitting error quantifies the degree to which the model's predicted distribution aligns with the target distribution. We define the fitting error of the model's predicted distribution at a specific input x and over the sample set s , with respect to \hat{Q} , as follows:

$$\begin{aligned} \mathcal{L}_F(\theta, \hat{Q}, x) &= \|p_{Y|x}(\theta) - \bar{Q}_{Y|x}\|_2^2, \\ \mathcal{L}_F(\theta, \hat{Q}, s) &= \mathbb{E}_{X \sim \hat{Q}_X} \|p_{Y|X}(\theta) - \hat{Q}_{Y|X}\|_2^2, \end{aligned} \quad (11)$$

where $p_{Y|x}(\theta) = (f_\theta(x))_{\Omega^*}^*$.

2. Uncertainty. Uncertainty refers to the inherent variability or randomness in the task for learning the true underlying conditional distribution $q_{Y|x}$. It is measured by the variance term $\text{Var}(Q_{Y|x}) = \mathbb{E}_{Q_{Y|x} \sim \mathcal{Q}_{Y|x}} \|Q_{Y|x} - \bar{Q}_{Y|x}\|_2^2$. Thus, the overall uncertainty across all possible features can be represented as

$$\mathbb{E}_{X \sim \hat{Q}_X} \text{Var}(Q_{Y|X}). \quad (12)$$

This uncertainty arises when the available data and information are insufficient to uniquely determine the underlying distribution, reflecting the intrinsic randomness inherent in the machine learning task. Its physical interpretation is similar to the cause of generalization error within the statistical machine learning framework, as both stem from limitations in sample size and insufficient information. Increasing the training sample size can help reduce both. However, they differ in their specific implications: generalization error represents the discrepancy between expected risk and empirical risk, which is difficult to calculate precisely, whereas uncertainty corresponds to the lower bound of the learning error proposed in our method, which can be accurately computed.

3. Gradient Norm. When using the Fenchel-Young Loss, the empirical risk in classification tasks takes the form $\mathbb{E}_{XY \sim \hat{Q}} d_\Omega(\mathbf{1}_Y, f_\theta(X))$. We thus define the gradient norm for an individual input x and the entire sample set s , respectively, as:

$$\begin{aligned} \mathcal{G}_\Omega(\theta, x) &:= \mathbb{E}_{Y \sim \hat{Q}_{Y|x}} \|\nabla_\theta d_\Omega(\mathbf{1}_Y, f_\theta(x))\|_2^2, \\ \mathcal{G}_\Omega(\theta, s) &:= \mathbb{E}_{XY \sim \hat{Q}} \|\nabla_\theta d_\Omega(\mathbf{1}_Y, f_\theta(X))\|_2^2. \end{aligned} \quad (13)$$

4. Structural Matrix. We define the structural matrix corresponding to the model f_θ and feature x as:

$$A_x := \nabla_\theta f_\theta(x)^\top \nabla_\theta f_\theta(x). \quad (14)$$

5. Structural Error. We define the structural error of f_θ with respect to feature x as follows:

$$S(\alpha, \beta, \gamma, A_x) = \alpha D(A_x) + \beta U(A_x) + \gamma L(A_x), \quad (15)$$

where:

$$\begin{aligned} U(A_x) &= -\log \lambda_{\min}(A_x), \\ L(A_x) &= -\log \lambda_{\max}(A_x), \\ D(A_x) &= U(A_x) - L(A_x). \end{aligned} \quad (16)$$

Here, α , β , and γ are positive real numbers representing the weights associated with $D(A_x)$, $U(A_x)$, and $L(A_x)$, respectively. Similarly, we define the structural error of the model f_θ on the sample set s as:

$$S(\alpha, \beta, \gamma, A_s) = \alpha D(A_s) + \beta U(A_s) + \gamma L(A_s), \quad (17)$$

where:

$$\lambda_{\min}(A_s) = \min_{(x,y) \in s} \lambda_{\min}(A_x), \quad \lambda_{\max}(A_s) = \max_{(x,y) \in s} \lambda_{\max}(A_x), \quad (18)$$

and $D(A_s) = U(A_s) - L(A_s)$.

5 Analysis of deep learning from the perspective of probability distribution estimation

This section will analyze deep learning using the Fenchel-Young Loss as the loss function, with the learning error as the optimization objective. More specifically, this section will demonstrate the following conclusions:

1. When using the Fenchel-Young Loss, the non-convex optimization mechanism in deep learning can be explained in terms of controlling the upper and lower bounds of the fitting error by reducing the gradient norm and the structural error.
2. Training a model with samples s and the SGD algorithm is equivalent to achieving the minimization of the fitting error $\mathcal{L}_F(\theta, \hat{Q}, s)$. Since \hat{Q} serves as an unbiased and consistent estimator of Q , this further translates into controlling the learning risk, i.e., $\min_\theta \mathcal{L}(\theta, s)$.
3. The lower bound of the learning risk $\mathcal{L}(\theta, s)$ is determined by the uncertainty, while its upper bound is given by the mutual information between the features and the labels.

5.1 Non-convex optimization mechanism

In this subsection, we will demonstrate that the optimization of the fitting error $\mathcal{L}_F(\theta, \hat{Q}, s)$ in deep learning is achieved by reducing its upper and lower bounds. The key factors within these bounds, namely the gradient norm and structural error, can be minimized through the use of the SGD algorithm and by adjusting the model architecture and the number of parameters, respectively.

We first establish the bounds of the fitting error $\mathcal{L}_F(\theta, \hat{Q}, s)$, which include the gradient norm and structural error as key components.

Theorem 5.1 . *Then, the following inequalities hold:*

$$\begin{aligned} e^{L(A_x)} \mathcal{G}_\Omega(\theta, x) - \text{Var}(\mathbf{1}_{Y|x}) &\leq \mathcal{L}_F(\theta, \hat{Q}, x) \leq e^{U(A_x)} \mathcal{G}_\Omega(\theta, x) - \text{Var}(\mathbf{1}_{Y|x}), \\ e^{L(A_s)} \mathcal{G}_\Omega(\theta, s) - \mathbb{E}_X \text{Var}(\mathbf{1}_{Y|x}) &\leq \mathcal{L}_F(\theta, \hat{Q}, s) \leq e^{U(A_s)} \mathcal{G}_\Omega(\theta, s) - \mathbb{E}_X \text{Var}(\mathbf{1}_{Y|x}). \end{aligned} \quad (19)$$

Here, $\text{Var}(\mathbf{1}_{Y|x}) = \mathbb{E}_{Y \sim \hat{Q}_{Y|x}} \|\mathbf{1}_Y - \hat{Q}_{Y|x}\|_2^2$, $(X, Y) \sim \hat{Q}$.

The proof of this theorem is provided in Appendix B.4.

The above theorem indicates that optimizing the fitting error $\mathcal{L}_F(\theta, \hat{Q}, s)$ can be achieved by reducing the gradient norm $\mathcal{G}_\Omega(\theta, s)$, along with $U(A_s)$ and $L(A_s)$. Since $U(A_s)$ and $L(A_s)$ constitute the structural error $S(\alpha, \beta, \gamma, A_s)$, our main conclusion is that non-convex optimization in deep learning is realized through minimizing both the gradient norm and the structural error. The SGD algorithm, with each iteration over samples, adjusts the parameters in a manner that tends towards the stationary points of the loss function for those samples [5, 6]. Therefore, SGD can effectively reduce the gradient norm $\mathcal{G}_\Omega(\theta, s)$.

Another factor influencing the model's prediction error is the structural error, denoted as $S(\alpha, \beta, \gamma, A_s)$. We demonstrate that structural error can be reduced by leveraging aspects such as the model's architecture (A_s), the number of parameters (α), and the independence among parameter gradients (γ). Our analysis is grounded in the following condition:

Definition 5.1 (Gradient Independence Condition) *Each column of $\nabla_{\theta} f$ is approximated as uniformly sampled from a ball $\mathcal{B}_\epsilon^{|\theta|} : \{x \in \mathbb{R}^{\theta}, \|x\|_2 \leq \epsilon\}$.*

This condition essentially posits that the gradients of the model’s output with respect to its parameters are approximately independent, without imposing strict limitations on the norm of the gradients. The independence of gradients implies a form of parameter independence, meaning that a slight change in one parameter has minimal impact on the final model output. We first explain the rationale for this assumption from an empirical and intuitive perspective. In models with a large number of parameters, each parameter has a sufficiently large solution space, naturally leading to weaker dependencies among parameters. Additionally, techniques such as dropout, random parameter initialization, and the inherent randomness in SGD all contribute to weakening the dependencies among parameters and bolstering the assumption of gradient independence. As the number of layers between parameters θ_i and θ_j increases, the dependence between $\nabla_{\theta_i} f_{\theta}(x)$ and $\nabla_{\theta_j} f_{\theta}(x)$ weakens [58]. Thus, increasing model depth helps to satisfy the Gradient Independence Condition. From an experimental perspective, for models without skip connections, in the experimental section 6, we observe that under conditions of large-scale parameter counts, the Gradient Independence Condition is generally satisfied immediately after the random initialization of the parameters. However, as the training process begins, both the parameters and their corresponding gradients undergo significant changes. During this phase, our experimental results suggest that this condition may no longer hold. As training continues and the model enters a more stable phase, the gradient norm becomes small at this stage, indicating that changes in the parameters have minimal impact on the model’s final output. Consequently, the experimental results imply that the Gradient Independence Condition becomes approximately valid again during this later phase of training. Therefore, this condition serves as a simplification of the model’s characteristics, which is reasonable and largely consistent with practical scenarios under certain circumstances. Below, we will derive a theorem based on this condition to describe how the number of parameters and inter-parameter correlations affect the structural error.

Theorem 5.2 *If the model satisfies the gradient independence condition 5.1 and $|\mathcal{Y}| \leq |\theta| - 1$, then with probability at least $1 - O(1/|\mathcal{Y}|)$ the following holds:*

$$\begin{aligned} L(A_x) &\leq U(A_x) \leq -\log\left(1 - \frac{2 \log |\mathcal{Y}|}{|\theta|}\right)^2 - \log \epsilon^2, \\ D(A_x) &= U(A_x) - L(A_x) \leq \log(Z(|\theta|, |\mathcal{Y}|) + 1), \end{aligned} \tag{20}$$

where $Z(|\theta|, |\mathcal{Y}|) = \frac{2|\mathcal{Y}|\sqrt{6 \log |\mathcal{Y}|}}{\sqrt{|\theta|-1}} \left(1 - \frac{2 \log |\mathcal{Y}|}{|\theta|}\right)^2$, is a decreasing function of $|\theta|$ and an increasing function of $|\mathcal{Y}|$.

The derivation for this theorem is presented in Appendix B.5. According to this theorem, the implementations to reduce structural error involve enhancing gradient independence to achieve the gradient independence condition 5.1 and reducing the structural error by increasing the number of parameters. **Random parameter initialization** allows the columns of the gradient matrix $\nabla_{\theta} f_{\theta}(x)$ to be approximately uniformly sampled from a ball. The stochasticity introduced by SGD helps to validate the gradient independence condition, thereby enabling control of the structural error through adjustments to the model’s parameter size and gradient norm. **Dropout** [59] effectively reduces the influence of these nodes on other parameters, thereby weakening the dependence among the columns of $\nabla_{\theta} f_{\theta}(x)$ and improving the rationality of the gradient independence condition. **Over-parameterization** not only enhances the model’s fitting capability but may also facilitate convergence to a smaller structural error as validated in Figure 7. **Skip connections** [11], in contrast to the aforementioned techniques, mitigate structural error by augmenting the elements of $\nabla_{\theta} f_{\theta}(x)$ without the need to satisfy the gradient independence condition, which is validated in Figure 5 and Figure 7.

Based on the above proofs and analysis, we propose a new perspective to understanding the non-convex optimization mechanisms in deep learning:

1. When using Fenchel-Young Loss, the model aims to fit the conditional probability distribution of labels given the features.
2. The optimization of the fitting error is achieved by reducing its upper and lower bounds. These bounds are influenced by two key factors: the gradient norm and the structural error. By controlling these elements, we can effectively minimize the fitting error.

3. The SGD algorithm plays a critical role in optimizing the gradient norm within these bounds. Through iterative updates based on stochastic gradients, SGD reduces the magnitude of the gradient norm, thereby tightening the bounds of the fitting error and facilitating convergence towards an optimal solution.

4. Structural error can be managed by carefully designing the model architecture (e.g., incorporating skip connections), adjusting the number of parameters, and employing specific parameter initialization methods. These strategies help in shaping the optimization landscape, making it easier to find better solutions and reduce structural errors. The conclusions outlined above are derived from theoretical analysis. To substantiate these findings with empirical evidence, we will conduct experimental validations in Section 6.

5.2 Sample size and learning error optimization

In the previous subsection, we demonstrated that mechanisms such as SGD and over-parameterization can reduce the fitting error $\mathcal{L}_F(\theta, \hat{Q}, s)$. In this subsection, we will theoretically show that, when the sample size is sufficiently large, reducing the fitting error $\mathcal{L}_F(\theta, \hat{Q}, s)$ aligns with optimizing the objective of this study, namely the learning error $\mathcal{L}(\theta, s)$. Additionally, in the absence of other prior information, smoothing \hat{Q} often improves the model's performance.

According to Proposition 4.1 and the definition of fitting error, the optimization problem for the learning error is equivalent to:

$$\min_{\theta} \mathcal{L}_F(\theta, \bar{Q}, s). \quad (21)$$

Since \hat{Q} is an unbiased and consistent estimator of \bar{Q} , it is evident that $\bar{Q} \approx \hat{Q}$ holds true when the size of the i.i.d. sample s is sufficiently large. Below, we provide a more rigorous proof.

Proposition 5.3 1. *As the sample size $n \rightarrow \infty$, the empirical distribution \hat{Q} converges to the true distribution \bar{Q} , and the uncertainty converges to 0:*

$$\begin{aligned} \lim_{n \rightarrow \infty} \hat{Q} &= \bar{Q} \\ \lim_{n \rightarrow \infty} \mathbb{E}_{X \sim \bar{Q}_X} \text{Var}(Q_{\mathcal{Y}|X}) &= 0. \end{aligned} \quad (22)$$

2. *For sufficiently large $n \gg 1$, $\bar{Q}_{\mathcal{Y}|x}$ can be approximated as:*

$$\bar{Q}_{\mathcal{Y}|x} \approx c \sum_{q_{\mathcal{Y}|x} \in \Delta^{|\mathcal{Y}|}} e^{-n D_{KL}(\hat{Q}_{\mathcal{Y}|x} \| q_{\mathcal{Y}|x})} q_{\mathcal{Y}|x}, \quad (23)$$

where $c = 1 / \sum_{q_{\mathcal{Y}|x} \in \Delta^{|\mathcal{Y}|}} e^{-n D_{KL}(\hat{Q}_{\mathcal{Y}|x} \| q_{\mathcal{Y}|x})}$ is a normalization constant.

The proof of this result is provided in Appendix B.6. The first conclusion of this theorem suggests that, as the sample size increases, learning based on the empirical distribution becomes equivalent to learning \bar{Q} , given a sufficiently large sample size. In this case, the uncertainty becomes negligible. At this point, the learning error is solely determined by the model's fitting error to the empirical distribution \hat{Q} , denoted as $\mathcal{L}_F(\theta, \hat{Q}, s)$. In other words, when the training sample size is sufficiently large, the model's performance is governed by its fitting capability. The second conclusion of the above theorem indicates that since \bar{Q} represents the posterior expectation of Q given the sample s , smoothing \hat{Q} to approximate \bar{Q} is justified in the absence of additional prior information (e.g., when the mapping from features to labels in the learning task is deterministic and there is no noise in the labels). This insight inspires the common practice of smoothing techniques, as exemplified by classical Laplacian smoothing.

5.3 Generalization capability and learning error

In this subsection, we prove the model-independent upper and lower bounds for the learning error. Based on these bounds, we will further discuss the generalization capability of models from the perspective of PD estimation.

First, we present a puzzling phenomenon: in highly imbalanced binary classification, such as when the ratio of positive to negative samples is 99:1 in both the training set and the overall data distribution. Suppose a model predicts all inputs as positive; in this case, the overall accuracy of the model is 99%, and the generalization error is 0. However, it is clear that the model is ineffective. Does this phenomenon suggest that **expressivity and generalization ability may not be sufficient to fully determine model performance?**

In the above scenario, the model does not change its output with varying input features and can only produce a constant vector. When the model’s predicted distribution matches \hat{Q}_Y , the fitting error $\mathcal{L}_F(\theta, \hat{Q}, s)$ reaches its minimum value, which is equal to $\text{Var}(\hat{Q}_{Y|X}) = \mathbb{E}_{X \sim \hat{Q}_X} \|\hat{Q}_{Y|x} - \bar{Q}_Y\|_2^2$. Therefore, if a trained model achieves a fitting error lower than $\text{Var}(\hat{Q}_{Y|X})$, it implies that the model possesses some predictive power beyond merely predicting the empirical mean of the labels. Conversely, if a model’s fitting error is not below this threshold, it suggests that the model may not have learned any meaningful patterns from the data and is essentially performing no better than a naive predictor that always outputs the average label. Based on this understanding, we define an effective model as follows:

Definition 5.2 (Effective Model) *If $\mathcal{L}_F(\theta, \hat{Q}, s) \leq \text{Var}(\hat{Q}_{Y|X})$, then we say the model f_θ is effective for \hat{Q} .*

This definition encapsulates the notion that for a model to be considered effective, it must at least perform better than a trivial model that always predicts the same constant vector (specifically, the mean of the target distribution). The model that predicts all inputs as positive, as introduced in the question at the beginning of this subsection, is evidently an ineffective model for \hat{Q} . Therefore, it is unnecessary to further discuss its performance.

To analyze the generalization capability of effective models, we present the following proposition:

Proposition 5.4 *If the model f_{θ_*} is an effective model for \bar{Q} , then we have:*

$$0 \leq \mathcal{L}(\theta_*, s) - \mathbb{E}_X[\text{Var}(q_{Y|X})] = \mathcal{L}_F(\theta_*, \bar{Q}, s) \leq \text{Var}(\bar{Q}_{Y|X}) \leq 2 \ln 2 I(X; Y), \quad (24)$$

where $(X, Y) \sim \bar{Q}$.

The proof of this theorem is provided in Appendix B.7. According to the definition, both $\text{Var}(\bar{Q}_{Y|X})$ and $I(X; Y)$ describe the expected distance between $\bar{Q}_{Y|x}$ and \bar{Q}_Y . Therefore, they can both be used to characterize the correlation between X and Y .

Based on Proposition 5.4, we can derive the following conclusions:

1. **Data determines the lower bound of the learning error.** For a fixed dataset s , regardless of the model used, the lower bound of the learning error (i.e., Uncertainty) always exists. According to Proposition 5.3, Uncertainty decreases as the sample size increases, eventually approaching zero.
2. **The mutual information between features and labels determines the upper bound of the learning error.** The stronger the correlation between features and labels, the higher the upper bound of the fitting error $\mathcal{L}_F(\theta_*, \bar{Q}, s)$. This indicates that models with stronger fitting capabilities are required when the mutual information is high.
3. **Higher correlation between features and labels leads to greater generalization error.** The higher the correlation between features and labels, the larger the difference $|\mathcal{L}_F(\theta_*, \bar{Q}, s) - \mathcal{L}_F(\theta_*, \hat{Q}, s)|$ between the model’s predicted distribution relative to the empirical distribution \hat{Q} and the true distribution \bar{Q} . This also implies that the expected generalization error is controlled by the mutual information between features and labels. Specifically, the higher the mutual information, the higher the expected generalization error.

6 Empirical Validation

Theorem 5.1 provides the foundation for reducing the fitting error of neural networks by controlling the gradient norm and structural error. In this section, we aim to validate the correctness of the core idea: non-convex optimization in deep learning is achieved by controlling the upper and lower bounds of the fitting error. Specifically, SGD reduces the gradient norm in the bounds, while over-parameterization, skip connections, and random parameter initialization in deep learning contribute to reducing the structural error.

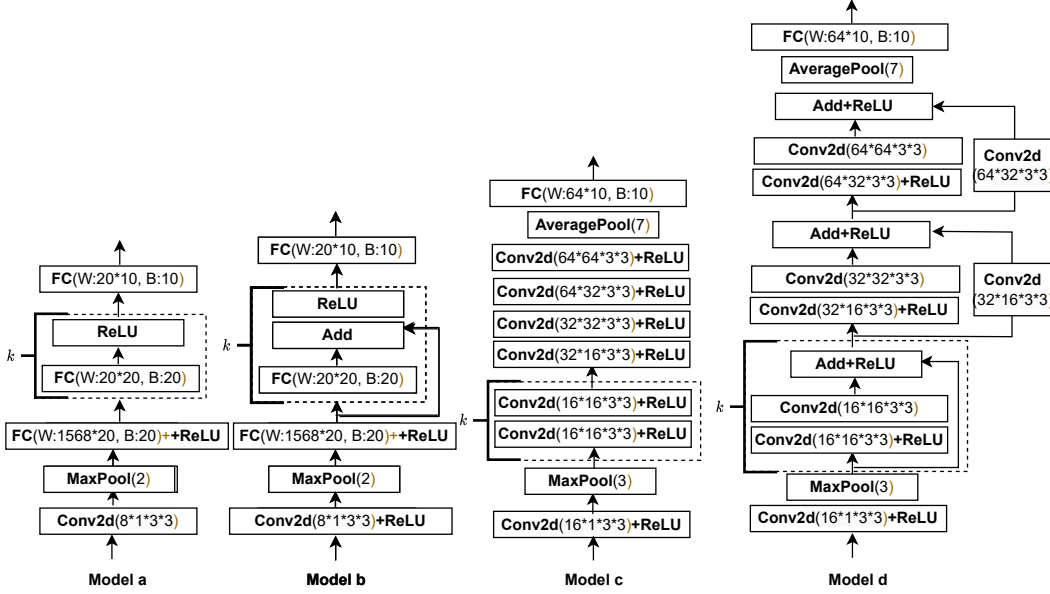


Figure 2: Model architectures and configuration parameters.

6.1 Experimental Configuration

Since the focus of this experiment is on evaluating whether models with different architectures align with the theoretical conclusions presented in this paper during the training process, rather than focusing on the final specific performance metrics or comparisons with existing algorithms, we primarily use the *MNIST* dataset [60] as a case study and design model architectures according to the conclusions to be verified. Model architectures and configuration parameters are illustrated in Figure 2. Models b and d extend Models a and c by incorporating skip connections, with k denoting the number of blocks (or layers), allowing for adjustable model depth. In the experiments, we control the parameter number by adjusting the model depth. To further verify the data-independence of the conclusions in this paper, we conducted experiments using the standard ResNet18[11] on CIFAR-10 [61] and Fashion MNIST [62]. The experiments were executed using the following computing environment: Python 3.7, Pytorch 2.2.2, and a GeForceRTX2080Ti GPU. The training parameters are as follows: the loss function is Softmax Cross-Entropy Loss, the batch size is 64, and the models were trained using the SGD algorithm with a learning rate of 0.01 and momentum of 0.9.

6.2 Verification of Bounds of Fitting Error

In this subsection, we design experiments to verify that the optimization process in deep learning operates as described in Theorem 5.1.

6.2.1 Experimental Design

According to Theorem 5.1, for any Ω , the gradient norm and structural error serve as upper and lower bounds for $\mathcal{L}_F(\theta, \hat{Q}, x)$. Therefore, during the process of training a model using SGD, we observe the trends of:

- $\log \mathcal{L}_F(\theta, \hat{Q}, x)$,
- the upper bound $U(A_x) + \log \mathcal{G}_\Omega(\theta, x)$,
- the lower bound $L(A_x) + \log \mathcal{G}_\Omega(\theta, x)$,
- $\log \mathcal{G}_\Omega(\theta, x)$,

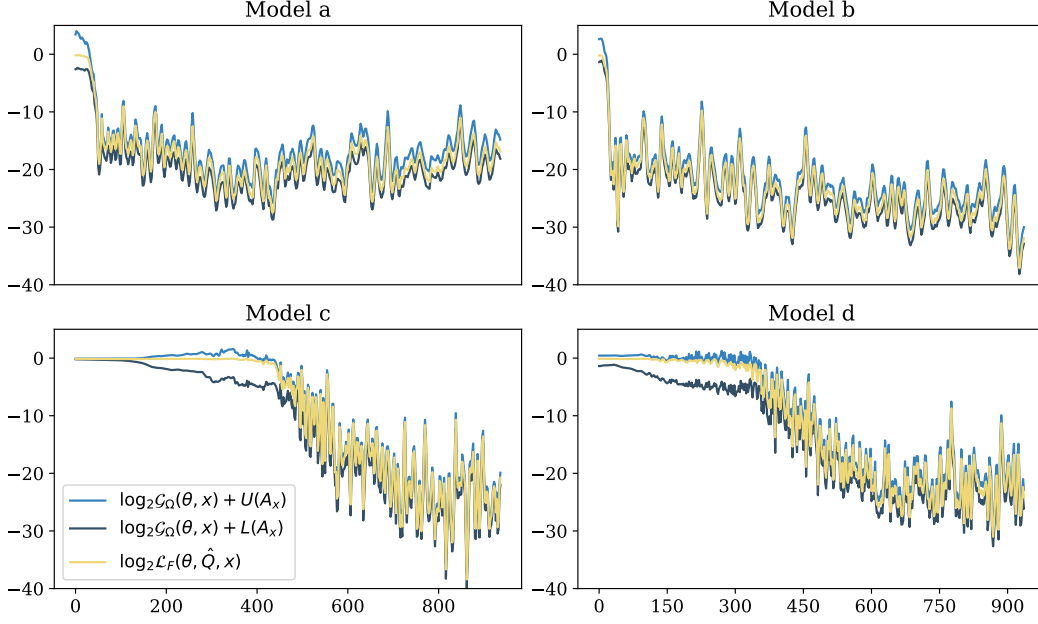


Figure 3: Changes of bounds during the training process.

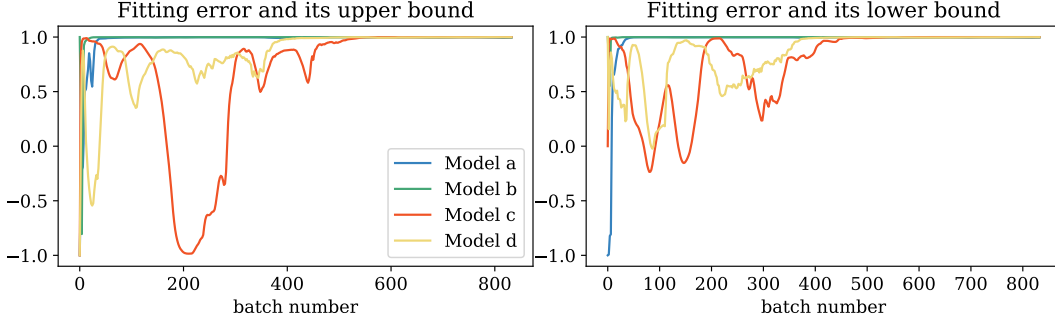


Figure 4: Local Pearson correlation coefficient curves during the training process.

to verify whether SGD optimizes by reducing the gradient norm, thereby controlling the upper and lower bounds of the fitting error $\mathcal{L}_F(\theta, \hat{Q}, x)$ as expected. The validation logic proceeds as follows:

1. If the upper and lower bounds of the $\mathcal{L}_F(\theta, \hat{Q}, x)$ diminish and converge towards zero during training, this outcome substantiates Theorem 5.1. This suggests that in deep learning, optimizing the loss function is achieved by minimizing both the gradient norm and the structural error. Specifically, the reduction in the upper and lower bounds of the loss is realized through the optimization of the gradient norm and structural error.

In this experiment, we assign a value of $k = 1$ to the models in Figure 2. To quantify the changes in correlations among these metrics as training progresses, we introduce the local Pearson correlation coefficient as a metric. Specifically, we apply a sliding window approach to compute the Pearson correlation coefficients between the given variables within each window. Let the sliding window length be m . Then, the local Pearson correlation coefficient between X and Y is given by:

$$r_w = \frac{\sum_{i=1}^m (X_i - \bar{X})(Y_i - \bar{Y})}{\sqrt{\sum_{i=1}^m (X_i - \bar{X})^2} \sqrt{\sum_{i=1}^m (Y_i - \bar{Y})^2}}, \quad (25)$$

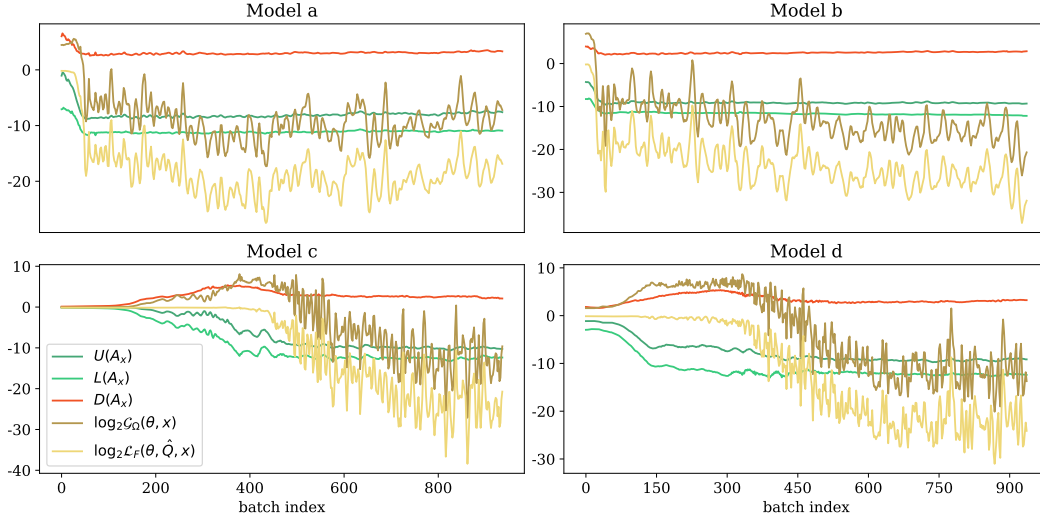


Figure 5: Changes in indicators during the training process.

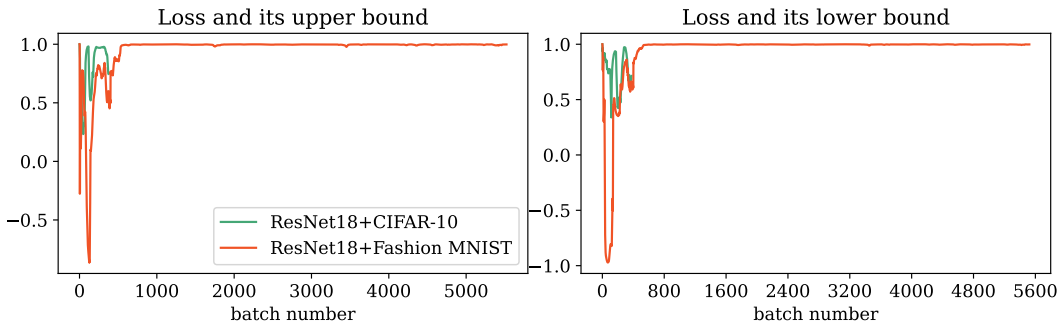


Figure 6: Local Pearson correlation coefficient curves for different datasets.

where $\bar{X} = \frac{1}{m} \sum_{i=1}^m X_i$ and $\bar{Y} = \frac{1}{m} \sum_{i=1}^m Y_i$. The local Pearson correlation coefficient ranges from -1 to 1. A coefficient value of 1 indicates that X and Y can be perfectly described by a linear equation, with all data points lying exactly on a straight line, and Y increases as X increases. A coefficient value of -1 indicates that all data points lie on a straight line, but Y decreases as X increases. A coefficient value of 0 indicates no linear relationship between the two variables. We use a sliding window of length 50 to compute the Pearson correlation coefficients between the loss and its upper and lower bounds.

6.2.2 Experimental Result

The fitting error, along with its respective bounds, is depicted in Figure 3. Additionally, the local Pearson correlation coefficients observed during training are illustrated in Figure 4 and Figure 6.

According to the experimental results, the upper bound $U(A_x) + \log \mathcal{G}_\Omega(\theta, x)$ and the lower bound $L(A_x) + \log \mathcal{G}_\Omega(\theta, x)$ decrease as training progresses, eventually converging close to 0. Simultaneously, the gap between these bounds narrows as training advances. Consequently, from a theoretical perspective, $\mathcal{L}_F(\theta, \hat{Q}, x)$ naturally follows this trend and approaches 0 as well. In the experimental results, the variation of $\mathcal{L}_F(\theta, \hat{Q}, x)$ increasingly aligns with the trends of its upper and lower bounds. This observation indicates that $\mathcal{L}_F(\theta, \hat{Q}, x)$ closely adheres to its theoretically established bounds. Furthermore, the reduction in the gap between the bounds signifies a decrease in uncertainty or variability surrounding the loss function. After the 500th epoch, the local Pearson correlation coefficients between $\mathcal{L}_F(\theta, \hat{Q}, x)$ and its upper and lower bounds approach 1 across all models. High Pearson correlation coefficients imply a strong linear relationship between $\mathcal{L}_F(\theta, \hat{Q}, x)$ and the theoretical

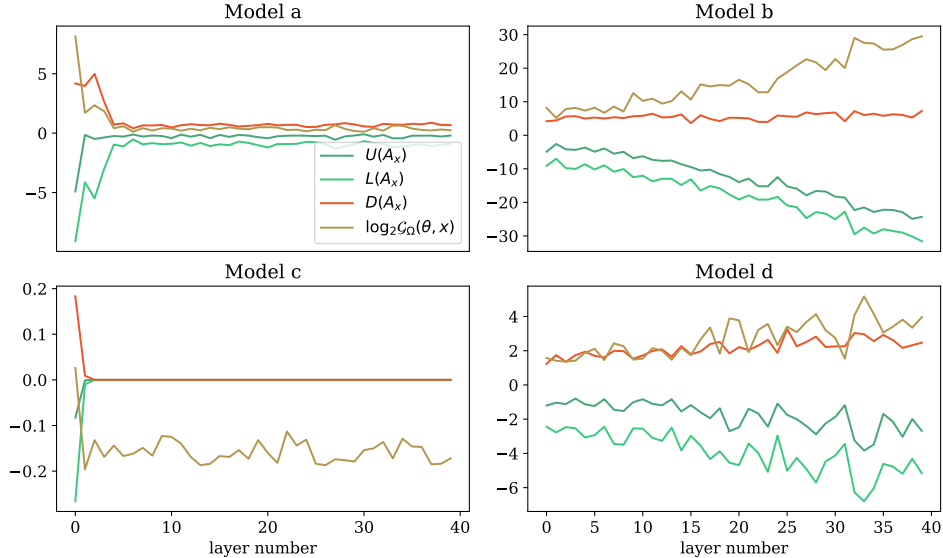


Figure 7: Changes in indicators during the increase in model depth.

bounds. This strong correlation further validates the tightness of these bounds. From an optimization perspective, reducing the upper and lower bounds of the loss constrains its maximum and minimum values, while narrowing the gap between these bounds ensures that the loss is closer to its minimum. The structural error introduced in this paper encompasses the control of both the upper and lower bounds as well as the gap between them, providing a comprehensive mechanism for loss optimization. Finally, Figure 6 shows that when using the standard ResNet18 and other datasets, the local Pearson correlation coefficients of $\mathcal{L}_F(\theta, \hat{Q}, x)$ with its upper and lower bounds also gradually converge to 1. This indicates that the above conclusions are independent of the dataset. These observations validate our explanation of the non-convex optimization mechanism in deep learning: non-convex optimization in deep learning is achieved by controlling the upper and lower bounds of the fitting error.

We further analyze the changes in structural error and gradient norm during the training process, as illustrated in Figure 5. As shown in the figure, the gradient norm generally exhibits a consistent downward trend as SGD iterations progress. This observation demonstrates that mini-batch SGD is effective in reducing the gradient norm. Additionally, we find that the ability of $\log \mathcal{G}_\Omega(\theta, x)$ to control the loss is closely related to whether the structural error converges to a small value. For instance, during the early stages of SGD iterations, in Model c and Model d, $\log \mathcal{G}_\Omega(\theta, x)$ increases while $U(A_x)$ and $L(A_x)$ decrease, yet the loss does not appear to be significantly affected by these changes. However, once $U(A_x)$, $L(A_x)$, and $D(A_x)$ converge, it becomes evident that both the loss and $\log \mathcal{G}_\Omega(\theta, x)$ exhibit a consistent downward trend. This suggests that the convergence of the structural error plays a crucial role in enabling the gradient norm to effectively influence and reduce the fitting error during training.

6.3 Verification on Structural Error Minimization

To validate the theoretical conclusions presented on structural error minimization in Subsection 5.1, we observe the changes in structural error during both the initialization phase and the training process by increasing the block number k .

6.3.1 Experimental Result on Initialization

Under the default initialization method (He initialization), the results of this experiment are illustrated in Figure 7. For Models a and c, which do not incorporate skip connections, as k increases, $U(A_x)$, $L(A_x)$, and $D(A_x)$ rapidly decrease, causing the structural error to decline and approach zero. This experimental result is fully consistent with the conclusions of 5.2. Skip connections in Models b and d amplify gradient values to prevent vanishing gradients. Therefore, both $U(A_x)$ and $L(A_x)$

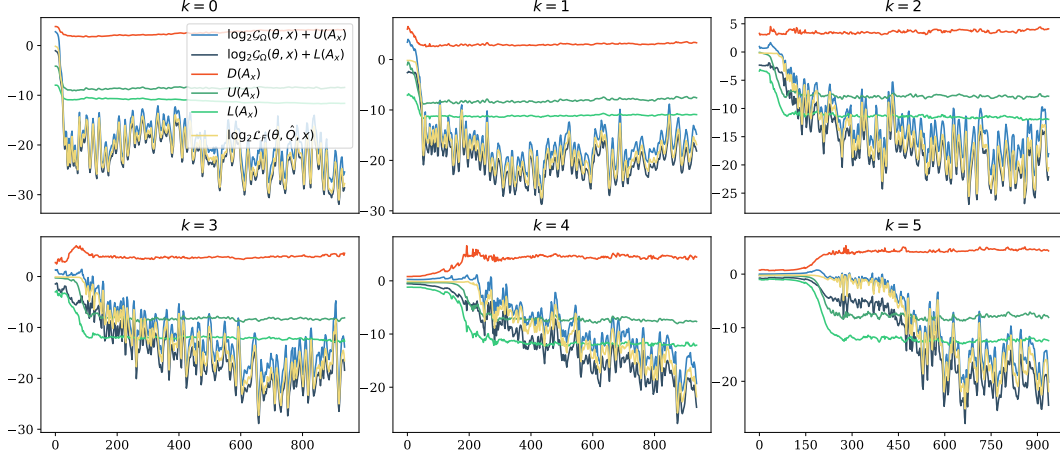


Figure 8: Bounds of model a with increasing blocks.

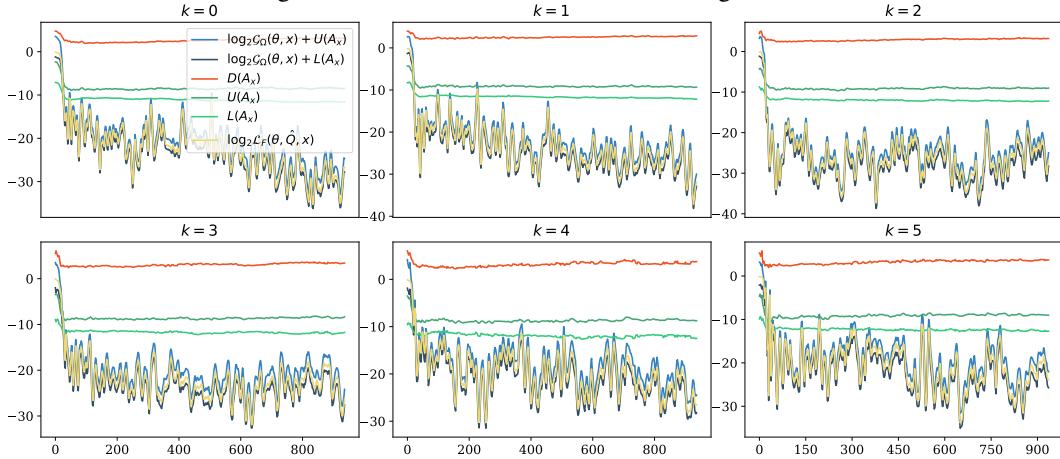


Figure 9: Bounds of model b with increasing blocks.

decrease, while $D(A_x)$ increases. Given that $U(A_x) \gg L(A_x)$, the structural error is primarily determined by $U(A_x)$, leading to a reduction in structural error. These experimental results confirm that skip connections reduce structural error by increasing the values of the elements in the structural matrix, thereby enlarging its extreme eigenvalues.

6.3.2 Experimental Results on Training Dynamics

We increase the value of k from 0 to 5 in Models a and b and train these models to investigate the impact of parameter number on training dynamics. The experimental results are illustrated in Figure 8 and Figure 9. To examine the correlation between the $\mathcal{L}_F(\theta, \hat{Q}, x)$ and its bounds, we also computed the local Pearson correlation coefficients using a sliding window of length 50. The results are shown in Figure 10 and Figure 11.

Below, we present the analysis of the experimental results and the conclusions drawn from them.

- **In the absence of skip connections, increasing parameter number prolongs the time required for structural error to converge, thereby delaying the onset of $\mathcal{L}_F(\theta, \hat{Q}, x)$ reduction.** As illustrated in Figure 8, as the number of layers k increases, the timing at which the $\mathcal{L}_F(\theta, \hat{Q}, x)$ of Model a begins to decrease corresponds to the point when structural error converges. Increasing parameter number prolongs the time required for structural error to converge, thereby delaying the onset of $\mathcal{L}_F(\theta, \hat{Q}, x)$ reduction. This observation aligns with Theorem 5.1, which implies that the optimization of empirical risk depends on controlling gradient norm and structural error.

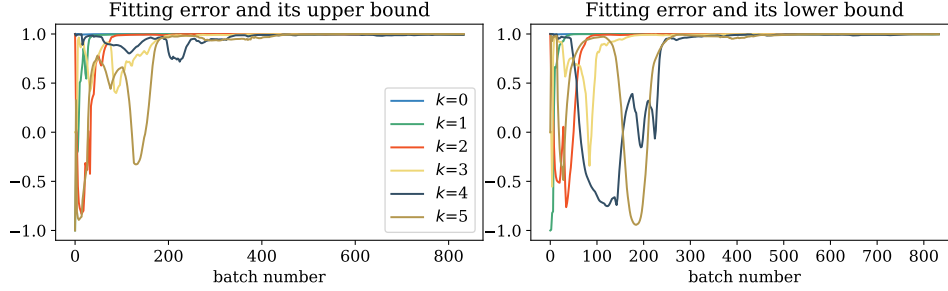


Figure 10: Local Pearson correlation coefficient curves of model a with increasing blocks.

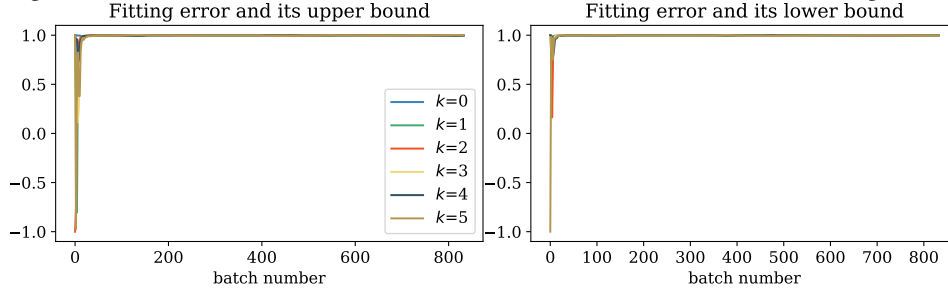


Figure 11: Local Pearson correlation coefficient curves of model b with increasing blocks.

- **Skip connections disrupt the initial Gradient Independence Condition but reduce the structural error by increasing the eigenvalues of the structural matrix.** At the onset of training, even with an increase in the number of layers, Model b does not exhibit a reduction in structural error. We attribute this primarily to the fact that skip connections disrupt the Gradient Independence Condition. Consequently, Theorem 5.2 is no longer applicable. However, the presence of skip connections addresses the vanishing gradient problem and reduces the structural error by increasing the eigenvalues of the structural matrix, thereby accelerating the model’s convergence as illustrated in Figure 10 and Figure 11.
- Regardless of whether skip connections are used, $U(A_x)$ and $L(A_x)$ converge to values near 2^{-10} , corresponding to $\lambda_{\max}(A_x)$ and $\lambda_{\min}(A_x)$ being around 2^{10} . We suspect that this phenomenon is related to the floating-point precision used by the training framework. However, further extensive experimentation is required to fully investigate and validate this hypothesis.

7 Conclusion

In this paper, we analyze machine learning tasks from the perspective of probability distribution estimation. Specifically, the conditional distribution of labels given features is modeled as a random variable, the learning error is formulated as the optimization objective, and the Fenchel-Young Loss is adopted as the loss function. We prove that, from the perspective of probability distribution estimation, although the optimization of the model’s fitting error is a typical non-convex optimization problem, it can be solved by reducing both the gradient norm and the structural error, which determine the upper and lower bounds of the fitting error. Furthermore, we show that SGD effectively reduces the gradient norm, while techniques such as over-parameterization, skip connections, and random parameter initialization contribute to reducing the structural error. Additionally, we establish model-independent upper and lower bounds on the learning error, providing new insights into the generalization capability of models. Finally, the core theoretical findings of this paper are validated through experiments. Our findings also suggest that precise error backpropagation is not strictly necessary in deep model optimization. Algorithms that directly target the gradient norm and structural error as optimization objectives may offer more efficient alternatives.

References

- [1] Carmon, Y., J. C. Duchi, O. Hinder, et al. Lower bounds for finding stationary points i. *Mathematical Programming*, 184:71 – 120, 2017.
- [2] Ghadimi, S., G. Lan. Stochastic first- and zeroth-order methods for nonconvex stochastic programming. *SIAM J. Optim.*, 23:2341–2368, 2013.
- [3] Nemirovski, A., A. B. Juditsky, G. Lan, et al. Robust stochastic approximation approach to stochastic programming. *SIAM J. Optim.*, 19:1574–1609, 2008.
- [4] Ge, R., F. Huang, C. Jin, et al. Escaping from saddle points - online stochastic gradient for tensor decomposition. *ArXiv*, abs/1503.02101, 2015.
- [5] Lee, J., M. Simchowitz, M. I. Jordan, et al. Gradient descent only converges to minimizers. In *Annual Conference Computational Learning Theory*. 2016.
- [6] Jentzen, A., B. Kuckuck, A. Neufeld, et al. Strong error analysis for stochastic gradient descent optimization algorithms. *Ima Journal of Numerical Analysis*, 2018.
- [7] Murty, K. G., S. N. Kabadi. Some np-complete problems in quadratic and nonlinear programming. Tech. rep., 1985.
- [8] Bellare, M., P. Rogaway. The complexity of approximating a nonlinear program. *Mathematical Programming*, 69:429–441, 1995.
- [9] Pardalos, P. M., S. A. Vavasis. Quadratic programming with one negative eigenvalue is np-hard. *Journal of Global optimization*, 1(1):15–22, 1991.
- [10] Nesterov, Y. How to advance in structural convex optimization. *OPTIMA: Mathematical Programming Society Newsletter*, 78:2–5, 2008.
- [11] He, K., X. Zhang, S. Ren, et al. Deep residual learning for image recognition. *2016 IEEE Conference on Computer Vision and Pattern Recognition (CVPR)*, pages 770–778, 2015.
- [12] Zhang, C., S. Bengio, M. Hardt, et al. Understanding deep learning requires rethinking generalization. *ArXiv*, abs/1611.03530, 2016.
- [13] Bottou, L., F. E. Curtis, J. Nocedal. Optimization methods for large-scale machine learning. *ArXiv*, abs/1606.04838, 2016.
- [14] Belkin, M., D. J. Hsu, S. Ma, et al. Reconciling modern machine-learning practice and the classical bias–variance trade-off. *Proceedings of the National Academy of Sciences*, 116:15849 – 15854, 2018.
- [15] Zhang, C., S. Bengio, M. Hardt, et al. Understanding deep learning (still) requires rethinking generalization. *Communications of the ACM*, 64:107 – 115, 2021.
- [16] Yun, C., S. Sra, A. Jadbabaie. Small nonlinearities in activation functions create bad local minima in neural networks. In *International Conference on Learning Representations*. 2018.
- [17] Du, S. S., X. Zhai, B. Póczos, et al. Gradient descent provably optimizes over-parameterized neural networks. *ArXiv*, abs/1810.02054, 2018.
- [18] Chizat, L., E. Oyallon, F. R. Bach. On lazy training in differentiable programming. In *Neural Information Processing Systems*. 2018.
- [19] Arjevani, Y., M. Field. Annihilation of spurious minima in two-layer relu networks. *ArXiv*, abs/2210.06088, 2022.
- [20] Jacot, A., F. Gabriel, C. Hongler. Neural tangent kernel: Convergence and generalization in neural networks. *ArXiv*, abs/1806.07572, 2018.
- [21] Du, S. S., J. Lee, H. Li, et al. Gradient descent finds global minima of deep neural networks. *ArXiv*, abs/1811.03804, 2018.
- [22] Zou, D., Y. Cao, D. Zhou, et al. Stochastic gradient descent optimizes over-parameterized deep relu networks. *ArXiv*, abs/1811.08888, 2018.
- [23] Arora, S., S. S. Du, W. Hu, et al. Fine-grained analysis of optimization and generalization for overparameterized two-layer neural networks. *ArXiv*, abs/1901.08584, 2019.

- [24] Mohamadi, M. A., W. Bae, D. J. Sutherland. A fast, well-founded approximation to the empirical neural tangent kernel. In *International Conference on Machine Learning*, pages 25061–25081. PMLR, 2023.
- [25] Wang, Y., D. Li, R. Sun. Ntk-sap: Improving neural network pruning by aligning training dynamics. *arXiv preprint arXiv:2304.02840*, 2023.
- [26] Sirignano, J. A., K. V. Spiliopoulos. Mean field analysis of neural networks: A central limit theorem. *Stochastic Processes and their Applications*, 2018.
- [27] Mei, S., A. Montanari, P.-M. Nguyen. A mean field view of the landscape of two-layer neural networks. *Proceedings of the National Academy of Sciences of the United States of America*, 115:E7665 – E7671, 2018.
- [28] Chizat, L., F. R. Bach. On the global convergence of gradient descent for over-parameterized models using optimal transport. *ArXiv*, abs/1805.09545, 2018.
- [29] Nguyen, P.-M., H. T. Pham. A rigorous framework for the mean field limit of multilayer neural networks. *Mathematical Statistics and Learning*, 6(3):201–357, 2023.
- [30] Selezнова, M., G. Kutyniok. Analyzing finite neural networks: Can we trust neural tangent kernel theory? In J. Bruna, J. S. Hesthaven, L. Zdeborová, eds., *Mathematical and Scientific Machine Learning, 16-19 August 2021, Virtual Conference / Lausanne, Switzerland*, vol. 145 of *Proceedings of Machine Learning Research*, pages 868–895. PMLR, 2021.
- [31] Dauphin, Y., R. Pascanu, Çağlar Gülçehre, et al. Identifying and attacking the saddle point problem in high-dimensional non-convex optimization. *ArXiv*, abs/1406.2572, 2014.
- [32] Keskar, N. S., D. Mudigere, J. Nocedal, et al. On large-batch training for deep learning: Generalization gap and sharp minima. *ArXiv*, abs/1609.04836, 2016.
- [33] Lee, J., I. Panageas, G. Piliouras, et al. First-order methods almost always avoid strict saddle points. *Mathematical Programming*, 176:311 – 337, 2019.
- [34] Zhou, Z., L. Li, P. Zhao, et al. Class-conditional sharpness-aware minimization for deep long-tailed recognition. In *Proceedings of the IEEE/CVF Conference on Computer Vision and Pattern Recognition*, pages 3499–3509. 2023.
- [35] Dinh, L., R. Pascanu, S. Bengio, et al. Sharp minima can generalize for deep nets. In *International Conference on Machine Learning*, pages 1019–1028. PMLR, 2017.
- [36] Vapnik, V. Statistical learning theory. *John Wiley & Sons google schola*, 2:831–842, 1998.
- [37] Bartlett, P. L., S. Mendelson. Rademacher and gaussian complexities: Risk bounds and structural results. *J. Mach. Learn. Res.*, 3:463–482, 2003.
- [38] Wu, Y. Statistical learning theory. *Technometrics*, 41:377–378, 2021.
- [39] Oneto, L., S. Ridella, D. Anguita. Do we really need a new theory to understand over-parameterization? *Neurocomputing*, 543:126227, 2023.
- [40] Hochreiter, S., J. Schmidhuber. Flat minima. *Neural Computation*, 9:1–42, 1997.
- [41] Jastrzebski, S., Z. Kenton, D. Arpit, et al. Three factors influencing minima in sgd. *ArXiv*, abs/1711.04623, 2017.
- [42] Lewkowycz, A., Y. Bahri, E. Dyer, et al. The large learning rate phase of deep learning: the catapult mechanism. *ArXiv*, abs/2003.02218, 2020.
- [43] Foret, P., A. Kleiner, H. Mobahi, et al. Sharpness-aware minimization for efficiently improving generalization. *ArXiv*, abs/2010.01412, 2020.
- [44] Neal, R. M., R. M. Neal. Priors for infinite networks. *Bayesian learning for neural networks*, pages 29–53, 1996.
- [45] Williams, C. K. I. Computing with infinite networks. In *Neural Information Processing Systems*. 1996.
- [46] Winther, O. Computing with finite and infinite networks. In *Neural Information Processing Systems*. 2000.
- [47] Neal, R. M. *Bayesian learning for neural networks*, vol. 118. Springer Science & Business Media, 2012.

- [48] Lee, J., Y. Bahri, R. Novak, et al. Deep neural networks as gaussian processes. *ArXiv*, abs/1711.00165, 2017.
- [49] Li, Y., Y. Liang. Learning overparameterized neural networks via stochastic gradient descent on structured data. *ArXiv*, abs/1808.01204, 2018.
- [50] Allen-Zhu, Z., Y. Li, Y. Liang. Learning and generalization in overparameterized neural networks, going beyond two layers. In *Neural Information Processing Systems*. 2018.
- [51] Allen-Zhu, Z., Y. Li, Z. Song. A convergence theory for deep learning via over-parameterization. *ArXiv*, abs/1811.03962, 2018.
- [52] Fu, S., D. Wang. Theoretical analysis of robust overfitting for wide dnns: An ntk approach. *ArXiv*, abs/2310.06112, 2023.
- [53] Seleznova, M., G. Kutyniok. Analyzing finite neural networks: Can we trust neural tangent kernel theory? In *Mathematical and Scientific Machine Learning, 16-19 August 2021, Virtual Conference / Lausanne, Switzerland*, vol. 145 of *Proceedings of Machine Learning Research*, pages 868–895. PMLR, 2021.
- [54] Vyas, N., Y. Bansal, G. Deepmind, et al. Empirical limitations of the ntk for understanding scaling laws in deep learning. *Trans. Mach. Learn. Res.*, 2023, 2023.
- [55] Nagarajan, V., J. Z. Kolter. Uniform convergence may be unable to explain generalization in deep learning. In *Neural Information Processing Systems*. 2019.
- [56] Todd, M. J. Convex analysis and nonlinear optimization: Theory and examples. jonathan m. borwein and adrian s. lewis, springer, new york, 2000. *International Journal of Robust and Nonlinear Control*, 13:92–93, 2003.
- [57] Blondel, M., A. F. T. Martins, V. Niculae. Learning with fenchel-young losses. *ArXiv*, abs/1901.02324, 2019.
- [58] Balduzzi, D., M. Frean, L. Leary, et al. The shattered gradients problem: If resnets are the answer, then what is the question? *ArXiv*, abs/1702.08591, 2017.
- [59] Krizhevsky, A., I. Sutskever, G. E. Hinton. Imagenet classification with deep convolutional neural networks. *Communications of the ACM*, 60:84 – 90, 2012.
- [60] LeCun, Y., L. Bottou, Y. Bengio, et al. Gradient-based learning applied to document recognition. *Proc. IEEE*, 86:2278–2324, 1998.
- [61] Krizhevsky, A., G. Hinton, et al. Learning multiple layers of features from tiny images. 2009.
- [62] Xiao, H., K. Rasul, R. Vollgraf. Fashion-mnist: a novel image dataset for benchmarking machine learning algorithms. *ArXiv*, abs/1708.07747, 2017.
- [63] Zhou, X. On the fenchel duality between strong convexity and lipschitz continuous gradient. *arXiv preprint arXiv:1803.06573*, 2018.
- [64] Kakade, S., S. Shalev-Shwartz, A. Tewari, et al. On the duality of strong convexity and strong smoothness: Learning applications and matrix regularization. *Unpublished Manuscript*, <http://ttic.uchicago.edu/shai/papers/KakadeShalevTewari09.pdf>, 2(1):35, 2009.
- [65] Cover, T. M. *Elements of Information Theory (Wiley Series in Telecommunications and Signal Processing)*. Elements of Information Theory (Wiley Series in Telecommunications and Signal Processing), 2017.
- [66] Csiszar, I. Information-type measures of difference of probability distributions and indirect observations. *Studia . Math. Hungar*, 2, 1967.
- [67] Kullback, S. A lower bound for discrimination information in terms of variation (corresp.). *IEEE Trans. Inf. Theory*, 13:126–127, 1967.
- [68] Csiszar, I., Z. Talata. Context tree estimation for not necessarily finite memory processes, via bic and mdl. *IEEE Transactions on Information Theory*, 52(3):1007–1016, 2006.
- [69] Blum, A., J. Hopcroft, R. Kannan. *Foundations of data science*. Cambridge University Press, 2020.
- [70] Cover, T. M., J. A. Thomas. *Elements of information theory (2. ed.)*. John Wiley & Sons, 2006.

- [71] Alabdali, O., A. Guessab, G. Schmeisser. Characterizations of uniform convexity for differentiable functions. *Applicable Analysis and Discrete Mathematics*, 2019.
- [72] Lin, G.-H., G.-H. Lin, M. Fukushima. Some exact penalty results for nonlinear programs and mathematical programs with equilibrium constraints. *Journal of Optimization Theory and Applications*, 118:67–80, 2003.
- [73] Niculescu, C., L.-E. Persson. *Convex functions and their applications*, vol. 23. Springer, 2006.
- [74] Noor, M. A., K. I. Noor. Higher order strongly general convex functions and variational inequalities. *AIMS Math*, 5(4):3646–3663, 2020.
- [75] Mohsen, B. B., M. A. Noor, K. I. Noor, et al. Strongly convex functions of higher order involving bifunction. *Mathematics*, 2019.
- [76] Zhu, D., P. Marcotte. Co-coercivity and its role in the convergence of iterative schemes for solving variational inequalities. *SIAM J. Optim.*, 6:714–726, 1996.
- [77] Noor, M. A., K. I. Noor. Properties of higher order preinvex functions. *Numerical Algebra, Control & Optimization*, 2021.
- [78] Seidler, J. Problem complexity and method efficiency in optimization. *Journal of the Operational Research Society*, 1984.
- [79] Nesterov, Y. Introductory lectures on convex optimization - a basic course. In *Applied Optimization*. 2014.
- [80] Zhang, J., T. He, S. Sra, et al. Why gradient clipping accelerates training: A theoretical justification for adaptivity. *arXiv: Optimization and Control*, 2019.
- [81] Zhang, B., J. Jin, C. Fang, et al. Improved analysis of clipping algorithms for non-convex optimization. *ArXiv*, abs/2010.02519, 2020.
- [82] Qian, J., Y. Wu, B. Zhuang, et al. Understanding gradient clipping in incremental gradient methods. In *International Conference on Artificial Intelligence and Statistics*. 2021.
- [83] Zhao, S.-Y., Y.-P. Xie, W.-J. Li. On the convergence and improvement of stochastic normalized gradient descent. *Science China Information Sciences*, 64, 2021.
- [84] Crawshaw, M., M. Liu, F. Orabona, et al. Robustness to unbounded smoothness of generalized signsgd. *Advances in neural information processing systems*, 35:9955–9968, 2022.
- [85] Reisizadeh, A., H. Li, S. Das, et al. Variance-reduced clipping for non-convex optimization. *ArXiv*, abs/2303.00883, 2023.
- [86] Chen, Z., Y. Zhou, Y. Liang, et al. Generalized-smooth nonconvex optimization is as efficient as smooth nonconvex optimization. In *International Conference on Machine Learning*. 2023.
- [87] Li, H., J. Qian, Y. Tian, et al. Convex and non-convex optimization under generalized smoothness. *ArXiv*, abs/2306.01264, 2023.
- [88] Darzentas, J. Problem complexity and method efficiency in optimization. *Journal of the Operational Research Society*, 35:455, 1983.
- [89] Arjevani, Y., Y. Carmon, J. C. Duchi, et al. Lower bounds for non-convex stochastic optimization. *Mathematical Programming*, 199:165–214, 2019.
- [90] Fang, C., C. J. Li, Z. Lin, et al. Spider: Near-optimal non-convex optimization via stochastic path integrated differential estimator. *ArXiv*, abs/1807.01695, 2018.
- [91] Nguyen, L. M., J. Liu, K. Scheinberg, et al. Sarah: A novel method for machine learning problems using stochastic recursive gradient. *ArXiv*, abs/1703.00102, 2017.
- [92] Wang, Z., K. Ji, Y. Zhou, et al. Spiderboost and momentum: Faster variance reduction algorithms. In *Neural Information Processing Systems*. 2019.
- [93] Cutkosky, A., F. Orabona. Momentum-based variance reduction in non-convex sgd. *ArXiv*, abs/1905.10018, 2019.

- [94] Zhou, D., P. Xu, Q. Gu. Stochastic nested variance reduction for nonconvex optimization. *ArXiv*, abs/1806.07811, 2018.
- [95] Lojasiewicz, S. Une propriété topologique des sous-ensembles analytiques réels. *Les équations aux dérivées partielles*, 117(87-89), 1963.
- [96] Kurdyka, K. On gradients of functions definable in o-minimal structures. In *Annales de l'institut Fourier*, vol. 48, pages 769–783. 1998.
- [97] Bolte, J., A. Daniilidis, A. Lewis. The łojasiewicz inequality for nonsmooth subanalytic functions with applications to subgradient dynamical systems. *SIAM Journal on Optimization*, 17(4):1205–1223, 2007.
- [98] Bolte, J., A. Daniilidis, A. Lewis, et al. Clarke subgradients of stratifiable functions. *SIAM Journal on Optimization*, 18(2):556–572, 2007.
- [99] Wang, X., Z. Wang. The exact modulus of the generalized concave kurdyka-łojasiewicz property. *Mathematics of Operations Research*, 47(4):2765–2783, 2022.
- [100] Attouch, H., J. Bolte. On the convergence of the proximal algorithm for nonsmooth functions involving analytic features. *Mathematical Programming*, 116:5–16, 2009.
- [101] Attouch, H., J. Bolte, P. Redont, et al. Proximal alternating minimization and projection methods for nonconvex problems: An approach based on the kurdyka-łojasiewicz inequality. *Mathematics of operations research*, 35(2):438–457, 2010.
- [102] Attouch, H., J. Bolte, B. F. Svaiter. Convergence of descent methods for semi-algebraic and tame problems: proximal algorithms, forward–backward splitting, and regularized gauss–seidel methods. *Mathematical programming*, 137(1):91–129, 2013.
- [103] Li, G., T. K. Pong. Douglas–rachford splitting for nonconvex optimization with application to nonconvex feasibility problems. *Mathematical programming*, 159:371–401, 2016.
- [104] Li, G., T. Pong. Calculus of the exponent of kurdyka-łojasiewicz inequality and its applications to linear convergence of first-order methods. *Foundations of Computational Mathematics*, page 1199–1232, 2018.
- [105] Li, M., K. Meng, X. Yang. Variational analysis of kurdyka-łojasiewicz property, exponent and modulus. *arXiv preprint arXiv:2308.15760*, 2023.
- [106] Gadat, S., F. Panloup. Optimal non-asymptotic bound of the ruppert-polyak averaging without strong convexity. *Tse Working Papers*, 2017.
- [107] Driggs, D., J. Tang, J. Liang, et al. Spring: A fast stochastic proximal alternating method for non-smooth non-convex optimization, 2021.
- [108] Fatkhullin, I., J. Etesami, N. He, et al. Sharp analysis of stochastic optimization under global kurdyka-łojasiewicz inequality. In S. Koyejo, S. Mohamed, A. Agarwal, D. Belgrave, K. Cho, A. Oh, eds., *Advances in Neural Information Processing Systems*, vol. 35, pages 15836–15848. Curran Associates, Inc., 2022.
- [109] Li, X., A. Milzarek, J. Qiu. Convergence of random reshuffling under the kurdyka-łojasiewicz inequality. *SIAM Journal on Optimization: A Publication of the Society for Industrial and Applied Mathematics*, 33(2):1092–1120, 2023.
- [110] —. Convergence of random reshuffling under the kurdyka-łojasiewicz inequality, 2023.
- [111] Fest, J.-B., A. Repetti, E. Chouzenoux. A stochastic use of the kurdyka-łojasiewicz property: Investigation of optimization algorithms behaviours in a non-convex differentiable framework, 2024.
- [112] Berner, J., P. Grohs, G. Kutyniok, et al. The modern mathematics of deep learning. *ArXiv*, abs/2105.04026, 2021.
- [113] Kelley, H. J. Gradient theory of optimal flight paths. *ARS Journal*, 30:947–954, 1960.
- [114] Dreyfus, S. E. The numerical solution of variational problems. *Journal of Mathematical Analysis and Applications*, 5:30–45, 1962.
- [115] Rumelhart, D. E., G. E. Hinton, R. J. Williams. Learning representations by back-propagating errors. *Nature*, 323:533–536, 1986.

- [116] Griewank, A., A. Walther. Evaluating derivatives - principles and techniques of algorithmic differentiation, second edition. In *Frontiers in applied mathematics*. 2000.
- [117] Robbins, H. E. A stochastic approximation method. *Annals of Mathematical Statistics*, 22:400–407, 1951.
- [118] Kiefer, J., J. Wolfowitz. Stochastic estimation of the maximum of a regression function. *Annals of Mathematical Statistics*, 23:462–466, 1952.
- [119] Lewicki, G., G. Marino. Approximation by superpositions of a sigmoidal function. *Zeitschrift Fur Analysis Und Ihre Anwendungen*, 22:463–470, 2003.
- [120] Ichi Funahashi, K. On the approximate realization of continuous mappings by neural networks. *Neural Networks*, 2:183–192, 1989.
- [121] Hornik, K., M. B. Stinchcombe, H. L. White. Multilayer feedforward networks are universal approximators. *Neural Networks*, 2:359–366, 1989.
- [122] Leshno, M., V. Y. Lin, A. Pinkus, et al. Original contribution: Multilayer feedforward networks with a nonpolynomial activation function can approximate any function. *Neural Networks*, 6:861–867, 1993.
- [123] Hoeffding, W. Probability inequalities for sums of bounded random variables. *The collected works of Wassily Hoeffding*, pages 409–426, 1994.
- [124] Valiant, L. G. A theory of the learnable. *Communications of the ACM*, 27(11):1134–1142, 1984.
- [125] Bousquet, O., A. Elisseeff. Stability and generalization. *Journal of Machine Learning Research*, 2:499–526, 2002.
- [126] Xu, H., S. Mannor. Robustness and generalization. *Machine Learning*, 86:391 – 423, 2010.
- [127] Belkin, M., A. Rakhlin, A. Tsybakov. Does data interpolation contradict statistical optimality? *ArXiv*, abs/1806.09471, 2018.
- [128] Geiger, M., A. Jacot, S. Spigler, et al. Scaling description of generalization with number of parameters in deep learning. *Journal of Statistical Mechanics: Theory and Experiment*, 2020, 2019.
- [129] Nakkiran, P., G. Kaplun, Y. Bansal, et al. Deep double descent: where bigger models and more data hurt. *Journal of Statistical Mechanics: Theory and Experiment*, 2021, 2019.
- [130] Rahman, S. M., M. O. Ahmad, M. Swamy. Bayesian wavelet-based image denoising using the gauss–hermite expansion. *IEEE Transactions on Image Processing*, 17(10):1755–1771, 2008.
- [131] Härdle, W., M. Müller, S. Sperlich, et al. *Nonparametric and semiparametric models*, vol. 1. Springer, 2004.
- [132] Sturges, H. A. The choice of a class interval. *Journal of the American Statistical Association*, 21(153):65–66, 1926.
- [133] Scott, D. W. On optimal and data-based histograms. *Biometrika*, 66(3):605–610, 1979.
- [134] Freedman, D., P. Diaconis. On the histogram as a density estimator: L₂ theory. *Zeitschrift für Wahrscheinlichkeitstheorie und verwandte Gebiete*, 57(4):453–476, 1981.
- [135] Parzen, E. On estimation of a probability density function and mode. *The Annals of Mathematical Statistics*, 33(3):1065–1076, 1962.
- [136] Silverman, B. W. *Density estimation for statistics and data analysis*. Routledge, 2018.
- [137] Hall, P., J. Racine, Q. Li. Cross-validation and the estimation of conditional probability densities. *Journal of the American Statistical Association*, 99(468):1015–1026, 2004.
- [138] McLachlan, G. J., S. X. Lee, S. I. Rathnayake. Finite mixture models. *Annual Review of Statistics and its Application*, 6:355–378, 2019.
- [139] Aldrich, J. R. A. Fisher and the making of maximum likelihood 1912–1922. *Statistical Science*, 12:162–176, 1997.
- [140] Hald, A. On the history of maximum likelihood in relation to inverse probability and least squares. *Statistical Science*, 14:214–222, 1999.

- [141] Meeker, W. Q., L. A. Escobar, F. G. Pascual. *Statistical methods for reliability data*. John Wiley & Sons, 2022.
- [142] Huber, P. J. Robust estimation of a location parameter. *Annals of Mathematical Statistics*, 35:492–518, 1964.
- [143] —. Robust regression: Asymptotics, conjectures and monte carlo. *Annals of Statistics*, 1:799–821, 1973.
- [144] MacKay, D. J. *Information theory, inference and learning algorithms*. Cambridge university press, 2003.
- [145] Sivia, D., J. Skilling. *Data analysis: a Bayesian tutorial*. OUP Oxford, 2006.
- [146] Murphy, K. P. *Probabilistic machine learning: an introduction*. MIT press, 2022.
- [147] Larochelle, H., I. Murray. The neural autoregressive distribution estimator. In *Proceedings of the fourteenth international conference on artificial intelligence and statistics*, pages 29–37. JMLR Workshop and Conference Proceedings, 2011.
- [148] Papamakarios, G., T. Pavlakou, I. Murray. Masked autoregressive flow for density estimation. *Advances in neural information processing systems*, 30, 2017.
- [149] Rezende, D., S. Mohamed. Variational inference with normalizing flows. In *International conference on machine learning*, pages 1530–1538. PMLR, 2015.
- [150] Dinh, L., J. Sohl-Dickstein, S. Bengio. Density estimation using real nvp. *arXiv preprint arXiv:1605.08803*, 2016.

A Definitions and lemmas

In this section, we outline the definitions and lemmas employed in this paper.

A.1 Legendre-Fenchel conjugate

Definition A.1 (Legendre-Fenchel conjugate) *The Legendre-Fenchel conjugate of a function Ω is denoted by*

$$\Omega^*(\nu) := \sup_{\mu \in \text{dom}(\Omega)} \langle \mu, \nu \rangle - \Omega(\mu).$$

By default, Ω is a continuous strictly convex function, and its gradient with respect to μ is denoted by μ_Ω^* . When $\Omega(\cdot) = \frac{1}{2} \|\cdot\|_2^2$, we have $\mu = \mu_\Omega^*$.

Lemma A.1 (Properties of Conjugate Duality) *The following are the properties of the Legendre-Fenchel conjugate [56]:*

1. $\Omega^*(\mu)$ is always a convex function of μ (independently of the shape of Ω).
2. The Fenchel-Young inequality holds:

$$\Omega(\mu) + \Omega^*(\nu) \geq \langle \mu, \nu \rangle \quad \forall \mu \in \text{dom}(\Omega), \nu \in \text{dom}(\Omega^*). \quad (26)$$

Equality is achieved when $\nu = \mu_\Omega^*$.

A.2 Fenchel-Young loss

Definition A.2 (Fenchel-Young loss) *The Fenchel-Young loss $d_\Omega: \text{dom}(\Omega) \times \text{dom}(\Omega^*) \rightarrow \mathbb{R}^+$ generated by Ω is defined as [57]:*

$$d_\Omega(\mu; \nu) := \Omega(\mu) + \Omega^*(\nu) - \langle \mu, \nu \rangle, \quad (27)$$

where Ω^* denotes the Legendre-Fenchel conjugate of Ω .

Lemma A.2 (Properties of Fenchel-Young losses) *The following are the properties of Fenchel-Young losses [57].*

1. $d_\Omega(\mu, \nu) \geq 0$ for any $\mu \in \text{dom}(\Omega)$ and $\nu \in \text{dom}(\Omega^*)$. If Ω is a lower semi-continuous proper convex function, then the loss is zero if and only if $\nu \in \partial\Omega(\mu)$. Furthermore, when Ω is strictly convex, the loss is zero if and only if $\nu = \mu_\Omega^*$.
2. $d_\Omega(\mu, \nu)$ is convex with respect to ν , and its subgradients include the residual vectors: $\nu_{\Omega^*}^* - \mu \in \partial_\nu d_\Omega(\mu, \nu)$. If Ω is strictly convex, then $d_\Omega(\mu, \nu)$ is differentiable and $\nabla_\nu d_\Omega(\mu, \nu) = \nu_{\Omega^*}^* - \mu$. If Ω is strongly convex, then $d_\Omega(\mu, \nu)$ is smooth, i.e., $\nabla_\nu d_\Omega(\mu, \nu)$ is Lipschitz continuous.

Table 1: Examples of common loss functions and their corresponding standard loss forms [57]

Loss	$\text{dom}(\Omega)$	$\Omega(\mu)$	$\hat{y}_\Omega(\theta)$	$d_\Omega(\theta; y)$
Squared	\mathbb{R}^d	$\frac{1}{2}\ \mu\ ^2$	θ	$\frac{1}{2}\ y - \theta\ ^2$
Perceptron	$\Delta^{ \mathcal{Y} }$	0	$\arg \max(\theta)$	$\max_i \theta_i - \theta_k$
Logistic	$\Delta^{ \mathcal{Y} }$	$-H(\mu)$	$\text{softmax}(\theta)$	$\log \sum_i \exp \theta_i - \theta_k$
Hinge	$\Delta^{ \mathcal{Y} }$	$\langle \mu, \mathbf{e}_k - \mathbf{1} \rangle$	$\arg \max(\mathbf{1} - \mathbf{e}_k + \theta)$	$\max_i [[i \neq k]] + \theta_i - \theta_k$
Sparsemax	$\Delta^{ \mathcal{Y} }$	$\frac{1}{2}\ \mu\ ^2$	$\text{sparsemax}(\theta)$	$\frac{1}{2}\ y - \theta\ ^2 - \frac{1}{2}\ \hat{y}_\Omega(\theta) - \theta\ ^2$
Logistic (one-vs-all) [0, 1]	$ \mathcal{Y} - \sum_i H([\mu_i, 1 - \mu_i])$		$\text{sigmoid}(\theta)$	$\sum_i \log(1 + \exp(-(2y_i - 1)\theta_i))$

¹ \mathbf{e}_i represents a standard basis ("one-hot") vector.

² $\hat{y}_\Omega \in \arg \min_{\mu \in \text{dom}(\Omega)} d_\Omega(\theta, \mu)$.

³ We denote the Shannon entropy by $H(p) := -\sum_i p_i \log p_i$, where $p \in \Delta^{\mathcal{Y}}$.

A.3 Strong Convexity and Lipschitz smoothness

Lemma A.3 Suppose $f : \mathbb{R}^n \rightarrow \mathbb{R}$ with the extended-value extension. The following conditions are all implied by strong convexity with parameter μ [63]:

1. $\frac{1}{2}\|s_x\|^2 \geq \mu(f(x) - f^*), \forall x$ and $s_x \in \partial f(x)$.
2. $\|s_y - s_x\| \geq \mu\|y - x\|, \forall x, y$ and any $s_x \in \partial f(x), s_y \in \partial f(y)$.
3. $f(y) \leq f(x) + s_x^T(y - x) + \frac{1}{2\mu}\|s_y - s_x\|^2, \forall x, y$ and any $s_x \in \partial f(x), s_y \in \partial f(y)$.
4. $(s_y - s_x)^T(y - x) \leq \frac{1}{\mu}\|s_y - s_x\|^2, \forall x, y$ and any $s_x \in \partial f(x), s_y \in \partial f(y)$.

Lemma A.4 For a function f with a Lipschitz continuous gradient over \mathbb{R}^n , the following relations hold [63]:

$$[5] \iff [7] \implies [6] \implies [0] \implies [1] \iff [2] \iff [3] \iff [4]$$

If the function f is convex, then all the conditions [0] – [7] are equivalent.

[0] $\|\nabla f(x) - \nabla f(y)\| \leq L\|x - y\|, \forall x, y$.

[1] $g(x) = \frac{L}{2}x^T x - f(x)$ is convex, $\forall x$.

[2] $f(y) \leq f(x) + \nabla f(x)^T(y - x) + \frac{L}{2}\|y - x\|^2, \forall x, y$.

[3] $(\nabla f(x) - \nabla f(y))^T(x - y) \leq L\|x - y\|^2, \forall x, y$.

[4] $f(\alpha x + (1 - \alpha)y) \geq \alpha f(x) + (1 - \alpha)f(y) - \frac{\alpha(1 - \alpha)L}{2}\|x - y\|^2, \forall x, y$ and $\alpha \in [0, 1]$.

[5] $f(y) \geq f(x) + \nabla f(x)^T(y - x) + \frac{1}{2L}\|\nabla f(y) - \nabla f(x)\|^2, \forall x, y$.

[6] $(\nabla f(x) - \nabla f(y))^T(x - y) \geq \frac{1}{L}\|\nabla f(x) - \nabla f(y)\|^2, \forall x, y$.

[7] $f(\alpha x + (1 - \alpha)y) \leq \alpha f(x) + (1 - \alpha)f(y) - \frac{\alpha(1 - \alpha)}{2L}\|\nabla f(x) - \nabla f(y)\|^2, \forall x, y$ and $\alpha \in [0, 1]$.

Lemma A.5 If f is strongly convex with parameter c , it follows that

$$f(y) \geq f(x) + \nabla f(x)^T(y - x) + \frac{c}{2}\|y - x\|^2, \quad \forall x, y. \quad (28)$$

If f is Lipschitz-smooth over \mathbb{R}^n , then it follows that

$$f(y) \leq f(x) + \nabla f(x)^T(y - x) + \frac{L}{2}\|y - x\|^2, \quad \forall x, y. \quad (29)$$

For the proofs of the above results, please refer to the studies [64, 63]. They further reveal the duality properties between strong convexity and Lipschitz smoothness as follows. For a function f and its Fenchel conjugate function f^* , the following assertions hold:

- If f is closed and strongly convex with parameter c , then f^* is Lipschitz smooth with parameter $1/c$.
- If f is convex and Lipschitz smooth with parameter L , then f^* is strongly convex with parameter $1/L$.

A.4 Lemmas

The theorems in this paper rely on the following lemmas.

Lemma A.6 (Pinsker's inequality) [65–67] *If p and q are probability densities/masses both supported on a bounded interval I , then we have*

$$D_{KL}(p\|q) \geq \frac{1}{2 \ln 2} \|p - q\|_1^2. \quad (30)$$

Lemma A.7 *If p and q are probability densities/masses both supported on a bounded interval I , then we have [68]*

$$D_{KL}(p, q) \leq \frac{1}{\inf_{x \in I} q(x)} \|p - q\|_2^2. \quad (31)$$

Lemma A.8 (Euler's Theorem for Homogeneous Functions) *If $f : \mathbb{R}^n \rightarrow \mathbb{R}$ is a differentiable k -homogeneous function, then*

$$x \cdot \nabla f(x) = kf(x),$$

where $x \cdot \nabla f(x) = \sum_{i=1}^n x_i \frac{\partial f}{\partial x_i}$.

Lemma A.9 *Suppose that we sample n points $x^{(1)}, \dots, x^{(n)}$ uniformly from the unit ball $\mathcal{B}_1^m : \{x \in \mathbb{R}^m, \|x\|_2 \leq 1\}$. Then with probability $1 - O(1/n)$ the following holds [69, Theorem 2.8]:*

$$\begin{aligned} \|x^{(i)}\|_2 &\geq 1 - \frac{2 \log n}{m}, \text{ for } i = 1, \dots, n. \\ |\langle x^{(i)}, x^{(j)} \rangle| &\leq \frac{\sqrt{6 \log n}}{\sqrt{m-1}} \text{ for all } i, j = 1, \dots, i \neq j. \end{aligned} \quad (32)$$

Lemma A.10 (Gershgorin's circle theorem) *Let A be a real symmetric $n \times n$ matrix, with entries a_{ij} . For $i = \{1, \dots, n\}$ let R_i be the sum of the absolute values of the non-diagonal entries in the i -th row: $R_i = \sum_{1 \leq j \leq n, j \neq i} |a_{ij}|$. For any eigenvalue λ of A , there exists $i \in \{1, \dots, n\}$ such that*

$$|\lambda - a_{ii}| \leq R_i. \quad (33)$$

Lemma A.11 (Sanov's theorem)

$$\lim_{n \rightarrow \infty} -\frac{1}{n} \log \Pr(\hat{q}|q) = D_{KL}(\hat{q}\|q), \quad (34)$$

where $D_{KL}(\hat{q}\|q)$ is Kullback-Leibler (KL) divergence [70, Theorem 11.4.1].

Lemma A.12 *Let A be an n -dimensional real symmetric matrix. Then, for any vector $e \in \mathbb{R}^n$, the following inequality holds:*

$$\lambda_{\min}(A) \|e\|_2^2 \leq e^\top A e \leq \lambda_{\max}(A) \|e\|_2^2. \quad (35)$$

The proof of this lemma is provided in Appendix B.1.

B Appendix for proofs

In this section, we prove the results stated in the paper and provide necessary technical details and discussions.

B.1 Proof of Lemma A.12

Lemma B.1 *Let A be an n -dimensional real symmetric matrix. Then, for any vector $e \in \mathbb{R}^n$, the following inequality holds:*

$$\lambda_{\min}(A)\|e\|_2^2 \leq e^\top A e \leq \lambda_{\max}(A)\|e\|_2^2. \quad (36)$$

Proof 1 *Here, we only prove the part concerning the maximum value. The proof for the minimum value is completely analogous.*

Since A is a real symmetric matrix, A has an orthonormal basis of eigenvectors e_1, \dots, e_n in \mathbb{R}^n .

This means that $Ae_i = \lambda_i(A)e_i$, where $\lambda_i(A)$ is the i -th eigenvalue of A , and $e_j^\top e_i = \begin{cases} 0, & i \neq j \\ 1, & i = j \end{cases}$.

Thus, for any vector $e = \sum_{i=1}^n k_i e_i$ in \mathbb{R}^n , we have:

$$\begin{aligned} e^\top A e &= \left(\sum_{j=1}^n k_j e_j^\top \right) A \left(\sum_{i=1}^n k_i e_i \right) \\ &= \left(\sum_{j=1}^n k_j e_j^\top \right) \left(\sum_{i=1}^n \lambda_i(A) k_i e_i \right) \\ &= \sum_{1 \leq i, j \leq n} \lambda_i(A) k_i k_j e_j^\top e_i \\ &= \sum_{i=1}^n \lambda_i(A) k_i^2 \quad (\text{since } e_j^\top e_i = 0 \text{ for } i \neq j) \\ &= \sum_{i=1}^n \lambda_{\max}(A) k_i^2 + \sum_{i=1}^n (\lambda_i(A) - \lambda_{\max}(A)) k_i^2 \\ &\leq \lambda_{\max}(A) \sum_{i=1}^n k_i^2 \quad (\text{since } \lambda_i(A) - \lambda_{\max}(A) \leq 0) \\ &= \lambda_{\max}(A) e^\top e. \end{aligned}$$

This completes the proof for the maximum value. The argument for the minimum value follows similarly by replacing $\lambda_{\max}(A)$ with $\lambda_{\min}(A)$.

B.2 Proof of Proposition 4.1

Proposition B.2

$$\mathcal{L}(\theta, s) = \mathbb{E}_{X \sim \bar{Q}_X} \text{Var}(Q_{Y|X}) + \mathbb{E}_{X \sim \bar{Q}_X} \|\bar{Q}_{Y|X} - p_{Y|X}(\theta)\|_2^2, \quad (37)$$

where $\text{Var}(Q_{Y|X}) = \mathbb{E}_{Q_{Y|X} \sim \mathcal{Q}_{Y|X}} \|Q_{Y|X} - \bar{Q}_{Y|X}\|_2^2$.

Proof 2 *Employing the Bias-Variance Decomposition, we obtain the following:*

$$\begin{aligned} \mathcal{L}(\theta, s) &= \mathbb{E}_{Q_X \sim \mathcal{Q}_X} \mathbb{E}_{X \sim Q_X} \mathbb{E}_{Q_{Y|X} \sim \mathcal{Q}_{Y|X}} \|Q_{Y|X} - p_{Y|X}(\theta)\|_2^2 \\ &= \mathbb{E}_{X \sim \bar{Q}_X} \left[\mathbb{E}_{Q_{Y|X} \sim \mathcal{Q}_{Y|X}} \|Q_{Y|X} - \bar{Q}_{Y|X}\|_2^2 + \|\bar{Q}_{Y|X} - p_{Y|X}(\theta)\|_2^2 \right] \\ &= \mathbb{E}_{X \sim \bar{Q}_X} \mathbb{E}_{Q_{Y|X} \sim \mathcal{Q}_{Y|X}} \|Q_{Y|X} - \bar{Q}_{Y|X}\|_2^2 + \mathbb{E}_{X \sim \bar{Q}_X} \|\bar{Q}_{Y|X} - p_{Y|X}(\theta)\|_2^2. \end{aligned} \quad (38)$$

B.3 Proof of Theorem 4.2

Theorem B.3 *Given that the loss function $\ell(q, p)$ satisfies the two conditions of strict convexity and optimal expectation, there exists a strictly convex function Ω such that:*

$$\ell(q, p) - \ell(q, q) = d_\Omega(q, p_\Omega^*). \quad (39)$$

Proof 3 *By setting $Q = \delta_q$, a Dirac delta distribution centered at q , it follows that $\mathbb{E}_{\omega \sim Q}[\ell(\omega, p)] = \ell(q, p)$. According to the expectation optimality condition, $\ell(q, p)$ achieves its global minimum value when $p = q$. Since $\ell(q, p)$ is continuous, differentiable, and strictly convex with respect to p , it possesses a unique minimum at $p = q$. At this point, the gradient of $\ell(q, p)$ with respect to p vanishes, i.e., $\nabla_p \ell(q, q) = 0$. Thus, we may express the gradient of the loss function as:*

$$\nabla_p \ell(q, p) = (p - q)^\top g(q, p), \quad (40)$$

where $g(q, p)$ is a vector-valued function that captures the direction and rate of change of the loss with respect to p .

Due to the uniqueness of the minimum value, the expected loss, $\mathbb{E}_{\omega \sim Q}[\ell(\omega, p)]$, is strictly convex, and at its minimum $\bar{\omega}$, where $\bar{\omega} = \mathbb{E}_{\omega \sim Q}[\omega]$, the gradient with respect to p vanishes, i.e., $\nabla_p \mathbb{E}_{\omega \sim Q}[\ell(\omega, \bar{\omega})] = 0$, which implies that $\sum_{\omega \in \mathcal{Q}} Q(\omega)(\bar{\omega} - \omega)^\top g(\omega, \bar{\omega}) = 0$, where $\omega \sim Q$.

Given that $Q(\omega)$ is an arbitrary distribution function, $g(\omega, p)$ must be independent of ω , allowing us to replace $g(\omega, p)$ with $g(p)$. Since $\mathbb{E}_{\omega \sim Q}[\ell(\omega, p)]$ is a strictly convex function, its Hessian with respect to p can be derived as:

$$\nabla_p^2 \mathbb{E}_{\omega \sim Q}[\ell(\omega, p)] = \sum_{\omega \in \mathcal{Q}} Q(\omega)[g(p) + (p - \omega)^\top \nabla_p g(p)]. \quad (41)$$

Simplifying, we get:

$$\nabla_p^2 \mathbb{E}_{\omega \sim Q}[\ell(\omega, p)] = g(p) + (p - \bar{\omega})^\top \nabla_p g(p) > 0. \quad (42)$$

The inequality above is derived from the fact that $\nabla_p^2 \mathbb{E}_{\omega \sim Q}[\ell(\omega, p)]$ is strictly convex.

When p is set to $\bar{\omega}$, we have $\nabla_p^2 \mathbb{E}_{\omega \sim Q}[\ell(\omega, p)] = g(\bar{\omega}) > 0$. Since $\bar{\omega}$ can take any value, it follows that for any arbitrary p , we get $g(p) > 0$.

Let us define a strictly convex function $\Omega(p)$ with its Hessian matrix given by $\nabla_p^2 \Omega(p) = g(p)$. The gradient of the loss function $\ell(q, p)$ with respect to p can be expressed as follows:

$$\begin{aligned} \nabla_p \ell(q, p) &= \nabla_p^2 \Omega(p)(p - q) \\ &= \nabla_p p_\Omega^* p - \nabla_p p_\Omega^* q \\ &= \nabla_p (\langle p, p_\Omega^* \rangle - \Omega(p)) - q^\top \nabla_p p_\Omega^* \\ &= \nabla_p (\Omega^*(p_\Omega^*) - \langle q, p_\Omega^* \rangle + h(q)). \end{aligned} \quad (43)$$

Since $\nabla_p \ell(q, q) = 0$, we find that $h(q) = \Omega^*(q_\Omega^*) - \langle q, q_\Omega^* \rangle + c = \Omega(q) + c$, where c is a constant. This leads to the following expression for the loss function:

$$\begin{aligned} \ell(q, p) &= \Omega^*(p_\Omega^*) - \langle q, p_\Omega^* \rangle + \Omega(q) + c, \\ \ell(q, q) &= c. \end{aligned} \quad (44)$$

It follows that:

$$\ell(q, p) - \ell(q, q) = d_\Omega(q, p_\Omega^*).$$

Theorem B.4 *Given that for all $x \in \mathcal{X}$, $\Omega^*(f_\theta(x)) = \min_\theta \Omega^*(f_\theta(x))$, it follows that there exist positive constants a , b , and ϵ such that: When $\theta \in \Theta'_\epsilon$, the norm $\|\theta\|_2$ controls the behavior of the function $\Omega^*(f_\theta(x))$ as follows:*

$$a\|\theta\|_2^2 \leq \Omega^*(f_\theta(x)) - \Omega^*(\mathbf{0}) \leq b\|\theta\|_2^2. \quad (45)$$

Proof 4 Since $\theta = \mathbf{0}$ represents the minimum point of $\Omega^*(f_\theta(x))$, it follows that $\forall \theta \in \Theta'_\epsilon$:

$$\begin{aligned}\nabla_\theta \Omega^*(f_\theta(x))|_{\theta=\mathbf{0}} &= \mathbf{0}, \\ \nabla_\theta^2 \Omega^*(f_\theta(x)) &\succeq 0, \\ \lambda_{\max}(\nabla_\theta^2 \Omega^*(f_\theta(x))) &\geq \lambda_{\min}(\nabla_\theta^2 \Omega^*(f_\theta(x))) \geq 0.\end{aligned}\tag{46}$$

By applying the mean value theorem, there exists $\theta' = \alpha \mathbf{0} + (1 - \alpha)\theta$, $\alpha \in [0, 1]$ such that the following inequalities hold:

$$\Omega^*(f_\theta(x)) = \Omega^*(f_{\mathbf{0}}(x)) + \theta^\top \nabla_\theta^2 \Omega^*(f_{\theta'}(x))\theta.\tag{47}$$

By applying Lemma A.12, we obtain the following inequality:

$$\lambda_{\min}(\nabla_\theta^2 \Omega^*(f_{\theta'}(x)))\|\theta\|_2^2 \leq \Omega^*(f_\theta(x)) - \Omega^*(\mathbf{0}) \leq \lambda_{\max}(\nabla_\theta^2 \Omega^*(f_{\theta'}(x)))\|\theta\|_2^2.\tag{48}$$

Let $a = \min_{\theta \in \Theta'_\epsilon} \lambda_{\min}(\nabla_\theta^2 \Omega^*(f_{\theta'}(x)))$ and $b = \max_{\theta \in \Theta'_\epsilon} \lambda_{\max}(\nabla_\theta^2 \Omega^*(f_{\theta'}(x)))$. Then, for all $\theta \in \Theta'_\epsilon$, we have:

$$a\|\theta\|_2^2 \leq \Omega^*(f_\theta(x)) - \Omega^*(\mathbf{0}) \leq b\|\theta\|_2^2.\tag{49}$$

B.4 Proof of Theorem 5.1

Theorem B.5 Let $\lambda_{\min}(A_s) = \min_{(x,y) \in s} \lambda_{\min}(A_x)$ and $\lambda_{\max}(A_s) = \max_{(x,y) \in s} \lambda_{\max}(A_x)$. Then, the following inequalities hold:

$$\begin{aligned}e^{L(A_x)} \mathcal{G}_\Omega(\theta, x) - \text{Var}(\mathbf{1}_{Y|x}) &\leq \mathcal{L}_F(\theta, \hat{Q}, x) \leq e^{U(A_x)} \mathcal{G}_\Omega(\theta, x) - \text{Var}(\mathbf{1}_{Y|x}), \\ e^{L(A_s)} \mathcal{G}_\Omega(\theta, s) - \mathbb{E}_X \text{Var}(\mathbf{1}_{Y|x}) &\leq \mathcal{L}_F(\theta, \hat{Q}, s) \leq e^{U(A_s)} \mathcal{G}_\Omega(\theta, s) - \mathbb{E}_X \text{Var}(\mathbf{1}_{Y|x}).\end{aligned}\tag{50}$$

Here, $\text{Var}(\mathbf{1}_{Y|x}) = \mathbb{E}_{Y \sim \hat{Q}_{Y|x}} \|\mathbf{1}_Y - \hat{Q}_{Y|x}\|_2^2$, $(X, Y) \sim \hat{Q}$.

Proof 5 We begin by recalling the definition of the Fenchel-Young Loss, which gives:

$$\|\nabla_\theta d_\Omega(\mathbf{1}_y, f_\theta(x))\|_2^2 = e_x^\top A_x e_x,\tag{51}$$

where $A_x = \nabla_\theta f_\theta(x)^\top \nabla_\theta f_\theta(x)$ and $e_x = \mathbf{1}_y - (f_\theta(x))_{\Omega^*}$.

From Lemma A.12, we have the following inequality:

$$\lambda_{\min}(A_x) \|\mathbf{1}_y - p_{Y|x}(\theta)\|_2^2 \leq \|\nabla_\theta d_\Omega(\mathbf{1}_y, f_\theta(x))\|_2^2 \leq \lambda_{\max}(A_x) \|\mathbf{1}_y - p_{Y|x}(\theta)\|_2^2,\tag{52}$$

where $p_{Y|x}(\theta) = (f_\theta(x))_{\Omega^*}$.

Taking the expectation over $Y \sim \hat{Q}_{Y|x}$, we obtain:

$$\begin{aligned}\lambda_{\min}(A_x) \left(\mathbb{E}_{Y \sim \hat{Q}_{Y|x}} \|\mathbf{1}_Y - \hat{Q}_{Y|x}\|_2^2 + \|\hat{Q}_{Y|x} - p_{Y|x}(\theta)\|_2^2 \right) \\ \leq \mathbb{E}_{Y \sim \hat{Q}_{Y|x}} \|\nabla_\theta d_\Omega(\mathbf{1}_Y, f_\theta(x))\|_2^2 \\ \leq \lambda_{\max}(A_x) \left(\mathbb{E}_{Y \sim \hat{Q}_{Y|x}} \|\mathbf{1}_Y - \hat{Q}_{Y|x}\|_2^2 + \|\hat{Q}_{Y|x} - p_{Y|x}(\theta)\|_2^2 \right).\end{aligned}\tag{53}$$

Since $\lambda_{\min}(A_x) \neq 0$, rearranging the terms in the inequality yields:

$$\begin{aligned}\frac{\mathbb{E}_{Y \sim \hat{Q}_{Y|x}} \|\nabla_\theta d_\Omega(\mathbf{1}_Y, f_\theta(x))\|_2^2}{\lambda_{\max}(A_x)} - \text{Var}(\mathbf{1}_{Y|x}) &\leq \|\hat{Q}_{Y|x} - p_{Y|x}(\theta)\|_2^2 \\ &\leq \frac{\mathbb{E}_{Y \sim \hat{Q}_{Y|x}} \|\nabla_\theta d_\Omega(\mathbf{1}_Y, f_\theta(x))\|_2^2}{\lambda_{\min}(A_x)} - \text{Var}(\mathbf{1}_{Y|x}),\end{aligned}\tag{54}$$

where $\text{Var}(\mathbf{1}_{Y|x}) = \mathbb{E}_{Y \sim \hat{Q}_{Y|x}} \|\mathbf{1}_Y - \hat{Q}_{Y|x}\|_2^2$.

Next, since $\lambda_{\min}(A_s) \neq 0$, $\lambda_{\min}(A_s) = \min_{x \in s} \lambda_{\min}(A_x)$, and $\lambda_{\max}(A_s) = \max_{x \in s} \lambda_{\max}(A_x)$, taking the expectation over $X \sim \hat{Q}_X$ leads to:

$$\begin{aligned}\frac{\mathbb{E}_{(X,Y) \sim \hat{Q}} \|\nabla_\theta d_\Omega(\mathbf{1}_Y, f_\theta(X))\|_2^2}{\lambda_{\max}(A_s)} \leq \mathbb{E}_{X \sim \hat{Q}_X} \|\hat{Q}_{Y|X} - p_{Y|X}(\theta)\|_2^2 - \mathbb{E}_X \text{Var}(\mathbf{1}_{Y|x}) \\ \leq \frac{\mathbb{E}_{(X,Y) \sim \hat{Q}} \|\nabla_\theta d_\Omega(\mathbf{1}_Y, f_\theta(X))\|_2^2}{\lambda_{\min}(A_s)},\end{aligned}\tag{55}$$

where $(X, Y) \sim \hat{Q}$.

Thus, the theorem is proven.

B.5 Proof of Theorem 5.2

Theorem B.6 *If the model satisfies the gradient independence condition 5.1 and $|\mathcal{Y}| \leq |\theta| - 1$, then with probability at least $1 - O(1/|\mathcal{Y}|)$ the following holds:*

$$\begin{aligned} L(A_x) &\leq U(A_x) \leq -\log\left(1 - \frac{2\log|\mathcal{Y}|}{|\theta|}\right)^2 - \log\epsilon^2, \\ D(A_x) &= U(A_x) - L(A_x) \leq \log(Z(|\theta|, |\mathcal{Y}|) + 1), \end{aligned} \quad (56)$$

where $Z(|\theta|, |\mathcal{Y}|) = \frac{2|\mathcal{Y}|\sqrt{6\log|\mathcal{Y}|}}{\sqrt{|\theta|-1}}\left(1 - \frac{2\log|\mathcal{Y}|}{|\theta|}\right)^2$, is a decreasing function of $|\theta|$ and an increasing function of $|\mathcal{Y}|$.

Since each column of $\nabla_\theta f_\theta(x)$ is uniformly from the ball $\mathcal{B}_\epsilon^{|\theta|} : \{x \in \mathbb{R}^{|\theta|}, \|x\|_2 \leq \epsilon\}$, according to Proposition A.9, then with probability $1 - O(1/|\mathcal{Y}|)$ the following holds:

$$\begin{aligned} A_{ii} &= \|\nabla_\theta(f_\theta(x))_i\|_2^2 \geq \left(1 - \frac{2\log|\mathcal{Y}|}{|\theta|}\right)^2 \epsilon^2, \text{ for } i = 1, \dots, |h|, \\ |A_{ij}| &= |\langle \nabla_\theta(f_\theta(x))_i, \nabla_\theta(f_\theta(x))_j \rangle| \leq \frac{\sqrt{6\log|\mathcal{Y}|}}{\sqrt{|\theta|-1}} \epsilon^2 \text{ for all } i, j = 1, \dots, |h|, i \neq j. \end{aligned} \quad (57)$$

Because $A = \nabla_\theta f_\theta(x)^\top \nabla_\theta f_\theta(x)$ is a symmetric positive semidefinite matrix, then we have $\lambda_{\min}(A_x) \leq A_{ii} \leq \lambda_{\max}(A_x)$. Then the following holds with probability $1 - O(1/|\mathcal{Y}|)$ at least

$$\begin{aligned} \lambda_{\min}(A_x) &\geq \left(1 - \frac{2\log|\mathcal{Y}|}{|\theta|}\right)^2 \epsilon^2, \\ \lambda_{\max}(A_x) &\leq \left(1 + \frac{2\log|\mathcal{Y}|}{|\theta|}\right)^2 \epsilon^2. \end{aligned} \quad (58)$$

According to Lemma A.10, there exist $k, k' \in \{1, \dots, |\mathcal{Y}|\}$

$$\begin{aligned} \lambda_{\max}(A_x) - A_{kk} &\leq R_k, \\ A_{k'k'} - \lambda_{\min}(A_x) &\leq R_{k'}, \end{aligned} \quad (59)$$

where $R_k = \sum_{1 \leq j \leq n, j \neq k} |A_{kj}|$, $R_{k'} = \sum_{1 \leq j \leq n, j \neq k'} |A_{k'j}|$. Based on the inequalities (57), we obtain

$$R_k + R_{k'} \leq 2(|\mathcal{Y}| - 1) \frac{\sqrt{6\log|\mathcal{Y}|}}{\sqrt{|\theta|-1}} \epsilon^2. \quad (60)$$

Since $A_{kk} \leq \epsilon^2$ and $|\mathcal{Y}| \leq |\theta| - 1$, then we have

$$\begin{aligned} \lambda_{\max}(A_x) - \lambda_{\min}(A_x) &\leq R_k + R_{k'} + A_{kk} - A_{k'k'} \\ &\leq R_k + R_{k'} + \epsilon^2 - A_{k'k'} \\ &\leq 2(|h| - 1) \frac{\sqrt{6\log|\mathcal{Y}|}}{\sqrt{|\theta|-1}} \epsilon^2 + \epsilon^2 - \left(1 - \frac{2\log|\mathcal{Y}|}{|\theta|}\right)^2 \epsilon^2 \\ &\leq 2(|\mathcal{Y}| - 1) \epsilon^2 \frac{\sqrt{6\log|\mathcal{Y}|}}{\sqrt{|\theta|-1}} + \frac{4\log|\mathcal{Y}|}{|\theta|} \epsilon^2 \\ &\leq \frac{2|\mathcal{Y}|\epsilon^2\sqrt{6\log|\mathcal{Y}|}}{\sqrt{|\theta|-1}}. \end{aligned} \quad (61)$$

By dividing both sides of the aforementioned inequality by the corresponding sides of inequalities (58), we obtain:

$$\frac{\lambda_{\max}(A_x)}{\lambda_{\min}(A_x)} \leq Z(|\theta|, |\mathcal{Y}|) + 1, \quad (62)$$

where $Z(|\theta|, |\mathcal{Y}|) = \frac{2|\mathcal{Y}|\sqrt{6\log|\mathcal{Y}|}}{\sqrt{|\theta|-1}}\left(1 - \frac{2\log|\mathcal{Y}|}{|\theta|}\right)^2$.

B.6 Proof of Proposition 5.3

Proposition B.7 1. As the sample size $n \rightarrow \infty$, the empirical distribution \hat{Q} converges to the true distribution \bar{Q} , and the uncertainty converges to 0:

$$\begin{aligned} \lim_{n \rightarrow \infty} \hat{Q} &= \bar{Q} \\ \lim_{n \rightarrow \infty} \mathbb{E}_{X \sim \bar{Q}_X} \text{Var}(Q_{Y|X}) &= 0. \end{aligned} \quad (63)$$

2. For sufficiently large $n \gg 1$, $\bar{Q}_{Y|x}$ can be approximated as:

$$\bar{Q}_{Y|x} \approx c \sum_{q_{Y|x} \in \Delta^{|Y|}} e^{-n D_{KL}(\hat{Q}_{Y|x} \| q_{Y|x})} q_{Y|x}, \quad (64)$$

where $c = 1 / \sum_{q_{Y|x} \in \Delta^{|Y|}} e^{-n D_{KL}(\hat{Q}_{Y|x} \| q_{Y|x})}$ is a normalization constant.

Proof 6 From Bayesian theory, the posterior probability of q given the data s is expressed as:

$$\Pr(q|s) = \frac{\Pr(\hat{Q}|q) \Pr(q)}{\Pr(\hat{Q})}. \quad (65)$$

Sanov's theorem A.11 provides an asymptotic characterization of the likelihood $\Pr(\hat{Q}|q)$ as:

$$\lim_{n \rightarrow \infty} -\frac{1}{n} \log \Pr(\hat{Q}|q) = D_{KL}(\hat{Q} \| q), \quad (66)$$

where $D_{KL}(\hat{Q} \| q)$ is the Kullback-Leibler (KL) divergence between the empirical distribution \hat{Q} and the candidate distribution q . Specifically: 1. If $q = \hat{Q}$, then $D_{KL}(\hat{Q} \| q) = 0$, and $\Pr(\hat{Q}|q) = 1$.

2. If $q \neq \hat{Q}$, then $D_{KL}(\hat{Q} \| q) > 0$, and $\Pr(\hat{Q}|q) = 0$. Thus, as $n \rightarrow \infty$, the posterior distribution $\Pr(q|s)$ collapses to a Dirac delta function centered at \hat{Q} :

$$\lim_{n \rightarrow \infty} \Pr(q|s) = \delta_{\hat{Q}}(q), \quad (67)$$

where $\delta_{\hat{Q}}(q)$ is the Dirac delta distribution. Based on the definition of uncertainty, $\text{Var}(Q_{Y|X}) = \mathbb{E}_{Q_{Y|X} \sim \mathcal{Q}_{Y|X}} \|Q_{Y|X} - \bar{Q}_{Y|X}\|_2^2$, it follows that:

$$\lim_{n \rightarrow \infty} \text{Var}(Q_{Y|X}) = 0. \quad (68)$$

Therefore, taking the expectation over the above expression yields:

$$\lim_{n \rightarrow \infty} \mathbb{E}_{X \sim \bar{Q}_X} \text{Var}(Q_{Y|X}) = 0. \quad (69)$$

The true distribution \bar{Q} is defined as the expectation of Q under the posterior distribution $\mathcal{Q}(q)$:

$$\bar{Q} = \mathbb{E}_{Q \sim \mathcal{Q}} Q. \quad (70)$$

As $n \rightarrow \infty$, the posterior distribution $\mathcal{Q}(q)$ converges to $\delta_{\hat{Q}}(q)$. Therefore:

$$\lim_{n \rightarrow \infty} \bar{Q} = \hat{Q}. \quad (71)$$

This proves the first part of the theorem.

For large but finite n , the posterior distribution $\mathcal{Q}(q_{Y|x})$ is not exactly a Dirac delta function but can be approximated as [70, Theorem 11.4.1]:

$$\mathcal{Q}(q_{Y|x}) \propto e^{-n D_{KL}(\hat{Q}_{Y|x} \| q_{Y|x})}. \quad (72)$$

Normalizing this distribution introduces the constant $c = 1 / \sum_{q_{Y|x} \in \Delta^{|Y|}} e^{-n D_{KL}(\hat{Q}_{Y|x} \| q_{Y|x})}$, leading to the approximation:

$$\bar{Q}_{Y|x} \approx c \sum_{q_{Y|x} \in \Delta^{|Y|}} e^{-n D_{KL}(\hat{Q}_{Y|x} \| q_{Y|x})} q_{Y|x}. \quad (73)$$

This completes the proof of the second part of the theorem.

B.7 Proof of Proposition 5.4

Proposition B.8 *If the model f_{θ_*} is an effective model for \bar{Q} , then we have:*

$$0 \leq \mathcal{L}(\theta_*, s) - \mathbb{E}_X[\text{Var}(q_{Y|X})] = \mathcal{L}_F(\theta_*, \bar{Q}, s) \leq \text{Var}(\bar{Q}_{Y|X}) \leq 2 \ln 2I(X; Y), \quad (74)$$

where $(X, Y) \sim \bar{Q}$.

Proof 7 Step 1.

Let v be a vector of dimension n . By the definition of norms, we know:

$$\|v\|_1^2 = \sum_{i=1}^n \sum_{j=1}^n |v_i| |v_j| \geq \sum_{i=1}^n |v_i|^2 = \|v\|_2^2. \quad (75)$$

This implies:

$$\|v\|_2^2 \leq \|v\|_1^2. \quad (76)$$

Applying this to the difference between $\bar{Q}_{Y|x}$ and $p_{Y|x}(\theta_*)$, we obtain:

$$\|\bar{Q}_{Y|x} - p_{Y|x}(\theta_*)\|_2^2 \leq \|\bar{Q}_{Y|x} - p_{Y|x}(\theta_*)\|_1^2. \quad (77)$$

Using Pinsker's inequality (Lemma A.6), which states that:

$$\|\bar{Q}_{Y|x} - p_{Y|x}(\theta_*)\|_1^2 \leq 2 \ln 2D_{KL}(\bar{Q}_{Y|x} \| p_{Y|x}(\theta_*)), \quad (78)$$

we can combine these results to conclude:

$$\|\bar{Q}_{Y|x} - p_{Y|x}(\theta_*)\|_2^2 \leq 2 \ln 2D_{KL}(\bar{Q}_{Y|x} \| p_{Y|x}(\theta_*)). \quad (79)$$

Step 2

From Theorem 4.1, under the assumption that there exists $x \in \mathcal{X}$ such that $(\bar{Q}_Y)_\Omega^* \in \mathcal{F}_\Theta(x)$, the loss function $\mathcal{L}(\theta, s)$ can be decomposed as:

$$\mathcal{L}(\theta_*, s) = \mathbb{E}_X[\text{Var}(q_{Y|X})] + \mathbb{E}_X[\|\bar{Q}_{Y|x} - p_{Y|x}(\theta_*)\|_2^2]. \quad (80)$$

Substituting the upper bound derived above for $\|\bar{Q}_{Y|x} - p_{Y|x}(\theta_*)\|_2^2$, we get:

$$\mathcal{L}(\theta_*, s) \leq \mathbb{E}_X[\text{Var}(q_{Y|X})] + \mathbb{E}_X[\|\bar{Q}_{Y|x} - \bar{Q}_Y\|_2^2]. \quad (81)$$

By definition, $\text{Var}(\bar{Q}_{Y|X}) = \mathbb{E}_{X \sim \bar{Q}_X} \|\bar{Q}_{Y|x} - \bar{Q}_Y\|_2^2$. Thus:

$$\mathcal{L}(\theta_*, s) \leq \mathbb{E}_X[\text{Var}(q_{Y|X})] + \text{Var}(\bar{Q}_{Y|X}). \quad (82)$$

Using inequality (79), we have:

$$\text{Var}(\bar{Q}_{Y|X}) \leq 2 \ln 2 \mathbb{E}_{X \sim \bar{Q}_X} [D_{KL}(\bar{Q}_{Y|x} \| \bar{Q}_Y)] = 2 \ln 2I(X; Y). \quad (83)$$

Thus, combining all terms, we conclude:

$$0 \leq \mathcal{L}(\theta_*, s) - \mathbb{E}_X[\text{Var}(q_{Y|X})] = \mathcal{L}_F(\theta_*, \bar{Q}, s) \leq \text{Var}(\bar{Q}_{Y|X}) \leq 2 \ln 2I(X; Y). \quad (84)$$

C Other related work

Strong convexity Strongly convex functions play a crucial role in optimization theory and related fields. For an exploration of the applications of strongly convex functions across various domains of pure and applied sciences, refer to the works cited in [71–77], as well as the references contained therein.

Lin et al. [72] were among the first to introduce the notion of higher-order strongly convex functions, applying this concept in the study of mathematical programs with equilibrium constraints. More specifically, a function F defined on a closed convex set K is deemed high-order strongly convex [72], provided there exists a constant $\mu \geq 0$ such that

$$F(u + t(v - u)) \leq (1 - t)F(u) + tF(v) - \mu\varphi(t)\|v - u\|^p, \quad \forall u, v \in K, t \in [0, 1], p \geq 1, \quad (85)$$

where $\varphi(t) = t(1 - t)$. It is noteworthy that when $p = 2$, high-order strongly convex functions revert to the conventional strongly convex functions, utilizing the same $\varphi(t)$ as defined in (85). Higher-order strongly generalized convex functions are instrumental in diverse fields, including engineering design, economic equilibrium, and multilevel games [75, 71, 74, 77].

Smoothness Classical textbook analyses of optimization problems [78, 79] frequently invoke the Lipschitz smoothness (Lipschitz-smoothness) condition. This condition stipulates that $\|\nabla^2 f(x)\| \leq L$ almost everywhere for some $L \geq 0$, where L is referred to as the smoothness constant. Such a condition paves the way for numerous crucial theoretical findings. For example, it is demonstrated that GD with a step size $h = 1/L$ achieves an optimal rate up to a constant factor for optimizing smooth non-convex functions [1]. A multitude of practical functions falls into this category, including quadratic and logistic functions, among others. Nevertheless, the Lipschitz-smoothness condition is relatively restrictive, being satisfied only by functions that are upper-bounded by quadratic functions. Functions that are Lipschitz-smooth cannot adequately model a diverse range of functions, such as higher-order polynomials and exponential functions. To overcome this limitation and offer a more inclusive model for optimization, prior research has introduced various concepts of generalized smoothness, which encompass a broader spectrum of functions utilized in machine learning applications. In this context, Zhang et al. [80] proposed the (L_0, L_1) -smoothness condition, a more general framework that assumes $\|\nabla^2 f(x)\| \leq L_0 + L_1 \|\nabla f(x)\|$ for certain constants $L_0, L_1 \geq 0$. This condition was motivated by their extensive experiments with language models. Subsequent studies have examined the (L_0, L_1) -smoothness condition [81–84], and explored variance reduction techniques for (L_0, L_1) -smooth functions [85]. Moreover, Chen et al. [86] introduced the notion of α -symmetric generalized smoothness, which is approximately as inclusive as the (L_0, L_1) -smoothness condition. Building on this, Li et al. [87] further generalized the (L_0, L_1) -smoothness condition to the ℓ -smoothness condition, which posits that $\|\nabla^2 f(x)\| \leq \ell(\|\nabla f(x)\|)$ for some non-decreasing continuous function ℓ .

Gradient-based optimization. The classical gradient-based optimization problems concerning standard Lipschitz smooth functions have been extensively studied for both convex [88, 79] and non-convex functions. In the convex scenario, the objective is to identify an ε -sub-optimal point x such that $f(x) - \inf_x f(x) \leq \varepsilon$. For convex Lipschitz-smooth problems, it has been established that GD attains a gradient complexity of $\mathcal{O}(1/\varepsilon)$. When dealing with strongly convex functions, GD achieves a complexity of $\mathcal{O}(\kappa \log(1/\varepsilon))$, where κ denotes the condition number. In the non-convex domain, the aim is to locate an ε -stationary point x satisfying $\|\nabla f(x)\| \leq \varepsilon$, given that identifying a global minimum is generally NP-hard. For deterministic non-convex Lipschitz-smooth problems, it is well-established that GD reaches the optimal complexity of $\mathcal{O}(1/\varepsilon^2)$, matching the lower bound presented in the paper [1]. Within the stochastic context, for an unbiased stochastic gradient with bounded variance, SGD achieves the optimal complexity of $\mathcal{O}(1/\varepsilon^4)$ [2, 89]. Fang et al. [90] introduced the first variance reduction algorithm, SPIDER, which attains the optimal sample complexity of $\mathcal{O}(\varepsilon^{-3})$ under the stronger expected smoothness assumption. Concurrently, several other variance reduction algorithms have been devised for stochastic non-convex optimization, achieving the optimal sample complexity, such as SARAH [91], SpiderBoost [92], STORM [93], and SNVRG [94]. For objective functions exhibiting (L_0, L_1) -smoothness, Zhang et al. [80] also put forth clipped GD and normalized GD, which maintain the optimal iteration complexity of $\mathcal{O}(1/\varepsilon^2)$, and proposed clipped SGD, which likewise achieves a sample complexity of $\mathcal{O}(1/\varepsilon^4)$. Zhang et al. [81] developed a general framework for clipped GD/SGD with momentum acceleration, achieving identical complexities for both deterministic and stochastic optimization. Reiszadeh et al. [85] managed to reduce the sample complexity to $\mathcal{O}(1/\varepsilon^3)$ by integrating the SPIDER variance reduction technique with gradient clipping. For objective functions characterized by ℓ -smoothness, Li et al. [87] achieve the same complexity for GD/SGD as under the classical Lipschitz-smoothness condition.

Non-convex optimization and Kurdyka-Łojasiewicz (KŁ) theory In the context of non-convex and non-smooth scenarios, the KŁ property is of significant importance and has been extensively studied in variational analysis and optimization. For an extended-real-valued function f and a point \bar{x} where f is finite and locally lower semicontinuous, the KŁ property of f at \bar{x} is characterized by the existence of some $\varepsilon > 0$ and $\nu \in (0, +\infty]$ such that the KŁ inequality

$$\psi'(f(x) - f(\bar{x}))d(0, \partial f(x)) \geq 1 \quad (86)$$

holds for all x satisfying $\|x - \bar{x}\| \leq \varepsilon$ and $f(\bar{x}) < f(x) < f(\bar{x}) + \nu$. Here, $d(0, \partial f(x))$ denotes the distance of 0 from the limiting subdifferential $\partial f(x)$ of f at x , and $\psi : [0, \nu) \rightarrow \mathbb{R}_+$, referred to as a desingularizing function, is assumed to be continuous, concave, and of class \mathcal{C}^1 on $(0, \nu)$, with $\psi(0) = 0$ and $\psi' > 0$ over $(0, \nu)$. The foundational work on the KŁ property originated from Łojasiewicz [95] and Kurdyka [96], who initially studied differentiable functions. Subsequently, the KŁ property was extended to nonsmooth functions in the work [97, 98]. By employing non-smooth

desingularizing functions, a generalized version of the concave KL property, along with its exact modulus, was introduced and studied by [99]. Among the widely used desingularizing functions is $\psi(s) := \frac{1}{\mu}s^{1-\theta}$, where $\theta \in [0, 1)$ is the exponent and $\mu > 0$ is the modulus. In this case, the corresponding KL inequality can be expressed as:

$$d(0, \partial f(x)) \geq \frac{\mu}{1-\theta} (f(x) - f(\bar{x}))^\theta. \quad (87)$$

The KL property, along with its associated exponent (especially the case when $\theta = 1/2$) and modulus, plays a pivotal role in estimating the local convergence rates of many first-order optimization algorithms. This connection has been extensively explored in the literature, including works such as [100–105], and references therein. Currently, there has been some research on the use of the KL property within a stochastic framework, and significant progress has been made [106–111]. These studies explore how the KL property can be leveraged to analyze stochastic, nonconvex optimization problems, providing valuable insights into the optimization mechanisms of such problems. However, directly applying the KL property to analyze the optimization mechanisms specific to deep learning remains rare.

C.1 Learning theory

We begin by offering a concise summary of the classical mathematical and statistical theory underlying machine learning tasks and algorithms, which, in their most general form, can be formulated as follows [112].

Definition C.1 (Learning task) *In a learning task, one is provided with a loss function $\ell : \mathcal{M}(\mathcal{X}, \mathcal{Y}) \times \mathcal{Z} \rightarrow \mathbb{R}$ and training data $s^n = \{z^{(i)}\}_{i=1}^n$ which is generated by independent and identically distributed (i.i.d.) sampling according to the unknown true distribution $Z \sim q$, where Z are random variables that take values in \mathcal{Z} . The objective is to construct a learning algorithm \mathcal{A} that utilizes training data s to find a model f_s that performs well on the entire data, where $f_s = \mathcal{A}(s) \in \mathcal{F}$, the hypothesis set $\mathcal{F} \subset \mathcal{M}(\mathcal{X}, \mathcal{Y})$, and the mapping $\mathcal{A} : s^n \rightarrow \mathcal{F}$. Here, performance is measured via $\mathbb{E}_Z[\ell(f_s, z)]$.*

To analyze the influencing factors of learning, the classical statistical machine learning framework introduces the optimization error (e_{opt}), generalization error (e_{gen}), and approximation error (e_{approx}).

The optimization error e_{opt} is primarily influenced by the algorithm \mathcal{A} that is used to find the model f_s in the hypothesis set \mathcal{F} for given training data s . By far, the gradient-based optimization methods are the most prevalent methods to address this issue, leveraging their ability to precisely and efficiently compute the derivatives by automatic differentiation in a lot of widely used models. Owing to the hierarchical structure of neural networks (NNs), the back-propagation algorithm has been proposed to efficiently calculate the gradient with respect to the loss function [113–116]. Stochastic gradient descent (SGD) [117] is a typical gradient-based optimization method used to identify the unique minimum of a convex function [118]. In scenarios where the objective function is non-convex, SGD generally converges to a stationary point, which may be either a local minimum, a local maximum, or a saddle point. Nonetheless, there are indeed conditions under which convergence to local minima is guaranteed [3–6].

The approximation error, e_{approx} , describes the model’s fitting capability. The universal approximation theorem [119–122] states that neural networks with only 2 layers can approximate any continuous function defined on a compact set up to arbitrary precision. This implies that the e_{approx} , decreases as the model complexity increases.

The generalization error, $e_{\text{gen}}(\mathcal{F})$, is defined as the difference between the true risk and the empirical risk. To bound the generalization error, Hoeffding’s inequality [123] alongside the union bound directly provides the PAC (Probably Approximately Correct) bound [124]. The uniform convergence bound represents a classic form of PAC generalization bound, which relies on metrics of complexity for the set \mathcal{F} , including the VC-dimension [38] and the Rademacher complexity [37]. Such bounds are applicable to all the hypotheses within \mathcal{F} . A potential drawback of the uniform convergence bounds is that they are independent of the learning algorithm, i.e., they do not take into account the way the hypothesis space is explored. To tackle this issue, algorithm-dependent bounds have been proposed to take advantage of some particularities of the learning algorithm, such as its uniform stability [125] or robustness [126].

However, the available body of evidence suggests that classical tools from statistical learning theory alone, such as uniform convergence, algorithmic stability, or bias-variance trade-off may be unable to fully capture the behavior of DNNs [12, 55]. The classical trade-off highlights the need to balance model complexity and generalization. While simpler models may suffer from high bias, overly complex ones can overfit noise (high variance). Reconciling the classical bias-variance trade-off with the empirical observation of good generalization, despite achieving zero empirical risk on noisy data using DNNs with a regression loss, presents a significant challenge [127]. Generally speaking, in deep learning, over-parameterization and perfectly fitting noisy data do not exclude good generalization performance. Moreover, empirical evidence across various modeling techniques, including DNNs, decision trees, random features, and linear models, indicates that test error can decrease even below the sweet-spot in the U-shaped bias-variance curve when further increasing the number of parameters [14, 128, 129]. Apart from inconsistencies with experiments, under the existing theoretical framework, the upper bound of the expected risk may be too loose. In other words, empirical risk and generalization ability may not completely determine model performance. A typical example is in highly imbalanced binary classification, such as when the ratio of positive to negative samples is 99:1. Suppose a model predicts all inputs as positive; in this case, the overall accuracy of the model is 99%, and the generalization error is 0, but clearly, the model is ineffective. Within the Definition C.1, the result learned by the model f_s is not completely deterministic and unique; it depends on the artificially chosen loss function, rather than being entirely determined by the data. This raises deeper questions: If the learning outcome depends on the artificial selection of the loss function, to what objects in the real physical world does the learned result correspond?

C.2 probability distribution estimation

In statistical data analysis, determining the probability density function (PDF) or probability mass function (PMF) from a limited number of random samples is a common task, especially when dealing with complex systems where accurate modeling is challenging. Generally, there are three main methods for this problem: parametric, semi-parametric, and non-parametric models.

Parametric models assume that the data follows a specific distribution with unknown parameters. Examples include the Gaussian model, Gaussian mixture models (GMMs), and distributions from the generalized exponential family. A major limitation of these methods is that they make quite simple parametric assumptions, which may not be sufficient or verifiable in practice [130]. Non-parametric models estimate the PDF/PMF based on data points without making assumptions about the underlying distribution [131]. Examples include the histogram [132–134] and kernel density estimation (KDE) [135–137]. While these methods are more flexible, they may suffer from overfitting or poor performance in high-dimensional spaces due to the curse of dimensionality. Semi-parametric models [138] strike a balance between parametric and non-parametric methods. They do not assume the a priori-shape of the PDF/PMF to estimate as non-parametric techniques. However, unlike the non-parametric methods, the complexity of the model is fixed in advance, in order to avoid a prohibitive increase of the number of parameters with the size of the dataset, and to limit the risk of overfitting. Finite mixture models are commonly used to serve this purpose.

Statistical methods for determining the parameters of a model conditional on the data, including the standard likelihood method [139–141], M-estimators [142, 143], and Bayesian methods [144–146], have been widely employed. However, traditional estimators struggle in high-dimensional space: because the required sample size or computational complexity often explodes geometrically with increasing dimensionality, they have almost no practical value for high-dimensional data.

Recently, neural network-based methods have been proposed for PDF/PMF estimation and have shown promising results in problems with high-dimensional data points such as images. There are mainly two families of such neural density estimators: auto-regressive models [147, 148] and normalizing flows [149, 150]. Autoregression-based neural density estimators decompose the density into the product of conditional densities based on probability chain rule $p(x) = \prod_i p(x_i|x_{1:i-1})$. Each conditional probability $p(x_i|x_{1:i-1})$ is modeled by a parametric density (e.g., Gaussian or mixture of Gaussians), and the parameters are learned by neural networks. Density estimators based on normalizing flows represent x as an invertible transformation of a latent variable z with a known density, where the invertible transformation is a composition of a series of simple functions whose Jacobian is easy to compute. The parameters of these component functions are then learned by neural networks.

D Notation Table

For ease of reference, we list the symbol variables defined in Table 2.

Table 2: Definitions and abbreviations of key variables.

$\partial f(x)$	sub-differential of a proper function f .
$ f(x) , \theta $	the length of vector $f(x)$ and the parameter number, respectively.
$\lambda_{\max}(A), \lambda_{\min}(A)$	the maximum and minimum eigenvalues of matrix A , respectively.
Ω^*	the Legendre-Fenchel conjugate of function Ω .
μ_{Ω}^*	the gradient of Ω at μ , i.e., $\mu_{\Omega}^* = \nabla \Omega^*(\mu)$.
$\mathcal{Z}, \mathcal{X}, \mathcal{Y}$	the instance space, the input feature space, and the label set, as defined in Subsection 3.2.
$q_{\mathcal{Z}}$ (abbreviated as q)	the unknown true distribution of the random pair Z (X, Y), with its support on \mathcal{Z} .
$q_{\mathcal{X}}, q_{\mathcal{Y} x}$	$q_{\mathcal{X}} := (q_{\mathcal{X}}(x_1), \dots, q_{\mathcal{X}}(x_{ \mathcal{X} }))^{\top}$, $q_{\mathcal{Y} x} := (q_{\mathcal{Y} x}(y_1 x), \dots, q_{\mathcal{Y} x}(y_{ \mathcal{Y} } x))^{\top}$.
$s^n(s)$	the n -tuple training dataset, consisting of i.i.d. samples drawn from the unknown true distribution q , as defined in Subsection 3.2.
$Q_{\mathcal{Z}}$ (abbreviated as Q)	the random variable in the probability simplex space Δ .
$\mathcal{Q}(s^n, \mathcal{P})$ (abbreviated as \mathcal{Q})	the posterior distribution of Q , conditional on s^n and the prior distribution \mathcal{P} .
$\mathcal{Q}_{\mathcal{X}}$ and $\mathcal{Q}_{\mathcal{Y} x}$	the posterior distributions of $Q_{\mathcal{X}}$ and $Q_{\mathcal{Y} x}$, respectively, given the sample s .
\bar{Q}	the posterior expectation of Q given s , as defined in Subsection 3.2.
\hat{Q}	the empirical PMF of Z , derived from these samples s^n , as defined in Subsection 3.2.
\mathcal{F}_{Θ}	the hypothesis space is a set of functions parameterized by Θ .
$f_{\theta}(x)$ ($f(x)$)	the model parameterized by θ .
$\mathbf{1}_y$	an indicator function that represents the one-hot encoding of the label y .
$\mathcal{L}(\theta, s)$	learning error, which describes the error between the model's predicted distribution and the plausible distributions under the posterior expectation given a sample s .
$\Omega^*(\nu)$	the Legendre-Fenchel conjugate of a function Ω .
$d_{\Omega}(\mu, \nu)$	the Fenchel-Young loss generated by Ω .
$p_{\mathcal{Y} x}(\theta)$	the model's predicted conditional probability distribution of Y given $X = x$: $p_{\mathcal{Y} x}(\theta) = (f_{\theta}(x))_{\Omega}^*$.
$\ell_{CE}(\cdot, \cdot)$	the Cross-Entropy Loss function.
$\mathcal{L}_F(\theta, \hat{Q}, x)$	fitting error on feature x , defined as $\mathcal{L}_F(\theta, \hat{Q}, x) = \ p_{\mathcal{Y} x}(\theta) - \hat{Q}_{\mathcal{Y} x}\ _2^2$,
$\mathcal{L}_F(\theta, \hat{Q}, s)$	fitting error on s , defined as $\mathcal{L}_F(\theta, \hat{Q}, s) = \mathbb{E}_{X \sim \hat{Q}_{\mathcal{X}}} \ p_{\mathcal{Y} X}(\theta) - \hat{Q}_{\mathcal{Y} X}\ _2^2$.
A_x	the structural matrix corresponding to the model with input x .
$S(\alpha, \beta, \gamma, A_x)$	the structural error of the model $f_{\theta}(x)$.
$U(A_x), L(A_x), D(A_x)$	$U(A_x) = -\log \lambda_{\min}(A_x)$, $L(A_x) = -\log \lambda_{\max}(A_x)$, $D(A_x) = U(A_x) - L(A_x)$.
α, β, γ	weights associated with $D(A_x)$, $U(A_x)$, and $L(A_x)$, respectively.
$\lambda_{\max}(A_s), \lambda_{\min}(A_s)$	$\lambda_{\min}(A_s) = \min_{x \in s} \lambda_{\min}(A_x)$, $\lambda_{\max}(A_s) = \max_{x \in s} \lambda_{\max}(A_x)$.
$\mathbb{E}_{X \sim \bar{Q}_{\mathcal{X}}} \text{Var}(Q_{\mathcal{Y} X})$	the uncertainty, where $\text{Var}(Q_{\mathcal{Y} x}) = \mathbb{E}_{Q_{\mathcal{Y} x} \sim \mathcal{Q}_{\mathcal{Y} x}} \ Q_{\mathcal{Y} x} - \bar{Q}_{\mathcal{Y} x}\ _2^2$.
$\mathcal{G}_{\Omega}(\theta, x)$	the gradient norm on feature x , defined as $\mathcal{G}_{\Omega}(\theta, x) := \mathbb{E}_{Y \sim \hat{Q}_{\mathcal{Y} x}} \ \nabla_{\theta} d_{\Omega}(\mathbf{1}_Y, f_{\theta}(x))\ _2^2$.
$\mathcal{G}_{\Omega}(\theta, s)$	the gradient norm on s , defined as $\mathcal{G}_{\Omega}(\theta, s) := \mathbb{E}_{X \sim \hat{Q}} \ \nabla_{\theta} d_{\Omega}(\mathbf{1}_Y, f_{\theta}(X))\ _2^2$.